SVEUČILIŠTE U SPLITU
FAKULTET ELEKTROTEHNIKE, STROJARSTVA I BRODOGRADNJE

POSLIJEDIPLOMSKI DOKTORSKI STUDIJ ELEKTROTEHNIKE I INFORMACIJSKIH TEHNOLOGIJA

KVALIFIKACIJSKI ISPIT

STOHASTIČKI PRISTUPI U RAČUNALNOM ELEKTROMAGNETIZMU – PRIMJENE U BIOELEKTROMAGNETIZMU

Anna Šušnjara

Split, 09. svibnja 2019.

UNIVERSITY OF SPLIT
FACULTY OF ELECTRICAL ENGINEERING, MECHANICAL ENGINEERING AND NAVAL ARCHITECTURE

POSTGRADUATE STUDY OF ELECTRICAL ENGINEERING AND INFORMATION TECHNOLOGY

QUALIFICATION EXAM

STOCHASTIC APPROACHES IN COMPUTATIONAL ELECTROMAGNETICS (CEM) – APPLICATIONS IN BIOELECTROMAGNETISM (BIOEM)

Anna Šušnjara

Split, 09. May 2019

CONTENTS

1. Introduction

Generally, mathematical and computational models in electromagnetism serve as a description of a physical system by using the mathematical concepts and language. Computer simulations are run based on a set of known input parameters in order to compute quantities of interest. A model may help to explain a system, to study the effects of different components, and to make predictions about its behaviour.

However, all computational model face two important issues. On one side the question is if the equations are solved correctly and on the other side if the equations being solved are correct. These two questions are tackled in the process of verification and validation of a computational model. The first one is related to a controllable procedure of building a model where it is possible to estimate the errors introduced by algorithms and mathematical description. The second question is associated with the lack of knowledge in the input parameters required for performing the analysis. Consequently, the uncertainties present in the input parameters are propagated to the related response. Uncertainty propagation (UP) techniques provide the mathematical description of the propagation of the uncertainties thus perfoming the uncertainty quantification (UQ) of the output variables.

The traditional uncertainty propagation methods rely upon the statistical approaches such as Monte Carlo sampling. These sampling based methods are easy to implement and very robust. However, they exhibit a slow convergence demanding a large number of samples to feed the deterministic solvers.

In the past few decades there has been a lot of effort to find the optimal uncertainty propagation technique. Contrary to statistical approaches the non-statistical based ones aim to represent the unknown stochastic solution as a function of random input variables. The nature of these methods can be intrusive or nonintrusive. The intrusiveness implies a more demanding implementation since new codes need to be developed, while the non-intrusive methods enable the use of previously validated deterministic models as black boxes in stochastic computations. Both approaches exhibit fast convergence and high accuracy under different conditions.

This work has two goals. The first one is to outline some of the most popular UQ/ UP methods in computational electromagnetics (CEM). Chapter 2 introduces some basic concepts of UQ framework and sensitivity analysis. The sensitivity analysis shows how the uncertainty in the output of a mathematical model or system can be apportioned to different sources of

uncertainty in its input parameters. This work investigates the “One-At-a-Time” (OAT) and the “Analysis Of Variance” (ANOVA) based approaches.

In three chapters to follow the basic concepts of three uncertainty propagation methods are given: generalized polynomial chaos (gPC), stochastic collocation method (SCM) and stochastic reduced order model (SROM) method.

The second goal of this work is to give an overview of the stochastic analysis reported so far in the area of computational electromagnetism (CEM). Chapter 6 is entirely dedicated to this review.

Finally, in chapter 7 a stochastic sensitivity analysis of bioheat transfer equation is presented in which the efficiency of the Stochastic Collocation versus Monte Carlo method is demonstrated.

2. Uncertainty quantification framework

Modelling the electromagnetic system can be viewed as the mathematical idealization of the physical processes governing its evolution. The process of building a mathematical model requires the definition of system geometry, material properties and the relationships between various quantities of interest. Rapid development of computer science enabled the numerical evaluation of approximated solutions of the mathematically described electromagnetic systems. However, it is important to question how confident we are about our models. Namely, there are two independent procedures that are used together for checking that a product, service, or system meets requirements and specifications and that it fulfils its intended purpose: the processes of verification and validation (V&V) [1]. The definitions for the V&V processes taken from the "*Guide for the Verification and Validation (V&V) of Computational Fluid Dynamics Simulations*" by The American Institute for Aeronautics and Astronautics (AIAA) in 1998 are as follows:

Verification – the process of determining that a model implementation accurately represents the developer's conceptual description of the model.

Validation – the process of determining the degree to which a model is an accurate representation of the real world for the intended uses of the model.

From the definitions it is obvious that the verification answers the question: "Are we solving the equations correctly?" which is a question coming from the mathematics' point of view [1]. The deficiencies between the mathematical idealization or algorithms and the actual physical process they represent can be recognized and measured as errors. The sources of errors can be the round-off, limited convergence of iterative algorithms, implementation mistakes (bugs), etc.

On the other hand, the validation is a process that answers the question: "Are we solving the correct equations?" which relates to the physics' point of view [1]. In this case the deficiency originates in our lack of knowledge about the input physical parameters required for performing the analysis. As such, the uncertainties can be divided into reducible and irreducible uncertainties. The uncertainty which can be reduced by increasing our knowledge, e.g. by performing more experimental investigations and/or developing new physical models is called *epistemic* or *systematic uncertainty*. On the other hand, the *aleatory* or *statistical uncertainty* cannot be reduced as it rises naturally from the observations of the system. Some additional experiments in this case can only be used to better characterise the variability.

The usual practice in the electromagnetic engineering is to use average values of input parameters thus leading to a rough representation of reality. However, the uncertainty present in input parameters can be quantified by using the statistical/ stochastic tools and propagated to the output value of interest via suitable uncertainty propagation method. The whole UQ framework is depicted in the Fig. 2.1.

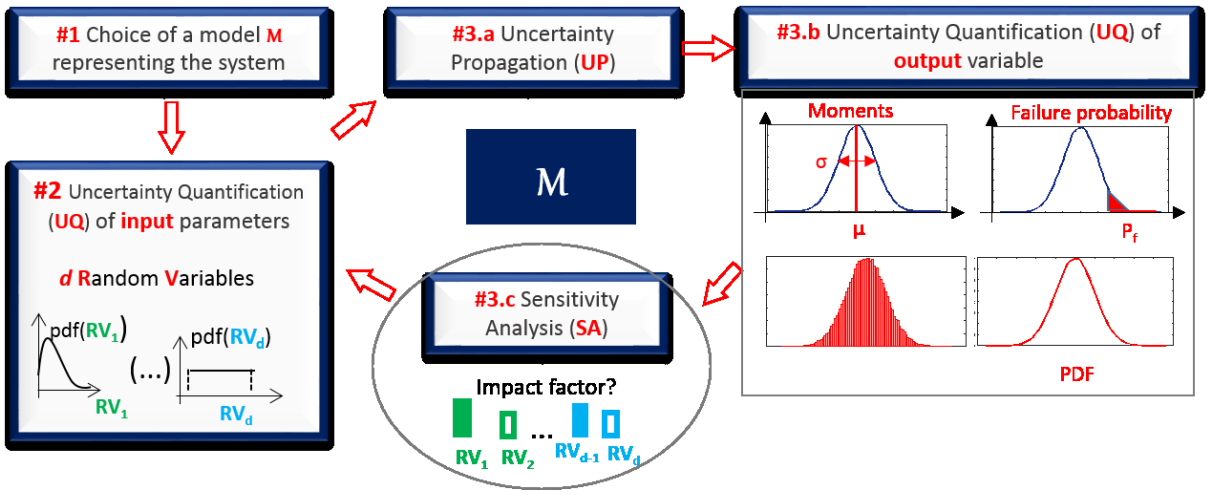

Figure 2.1. The uncertainty quantification (UQ) framework

2.1.Uncertainty quantification (UQ) of model input parameters

The parameters with uncertainties are identified and represented in terms of random variables/ fields. Based on the available information, the UQ of the input parameters can be done by using the direct methods such as experimental observations, theoretical arguments or expert opinions, or by using the inverse methods such as the inference, calibration, etc [1]. The UQ of input parameters is a demanding task and the detailed discussion related to its theory and approaches is out of the scope of this work. A review of available tools can be found elsewhere, e.g. in [2] - [4].

For the majority of scenarios encountered in the area of CEM the input parameters are modelled as random variables (RV) attributed with the corresponding standard probability density function (pdf). Furthermore, in many CEM applications the variables are assumed to be independent. In this work a random input variable is denoted by X. If there are more than one random input parameters, a vector of d random input parameters is formed:

$$\boldsymbol{X} = [X_1, \ldots, X_d]$$

Since in practice RVs which represent the input parameters are usually not standardized, the random vector $\boldsymbol{X}$ has to be transformed into a set of reduced variables through an isoprobabilistic transform [5]. Depending on the marginal distribution of each input variable X_k, $k = 1, \ldots d$, the associated reduced variable may be standard normal: $\xi \sim N(0,1)$, standard uniform: $\xi \sim U(-1,1)$, or some other variable with standard distribution. Thus, the resulting vector of input parameters is denoted by:

$$\boldsymbol{\xi} = [\xi_1, \ldots, \xi_d]$$

Figure 2.2. shows the random variables with three typical standard distributions, uniform, normal, and beta, respectively.

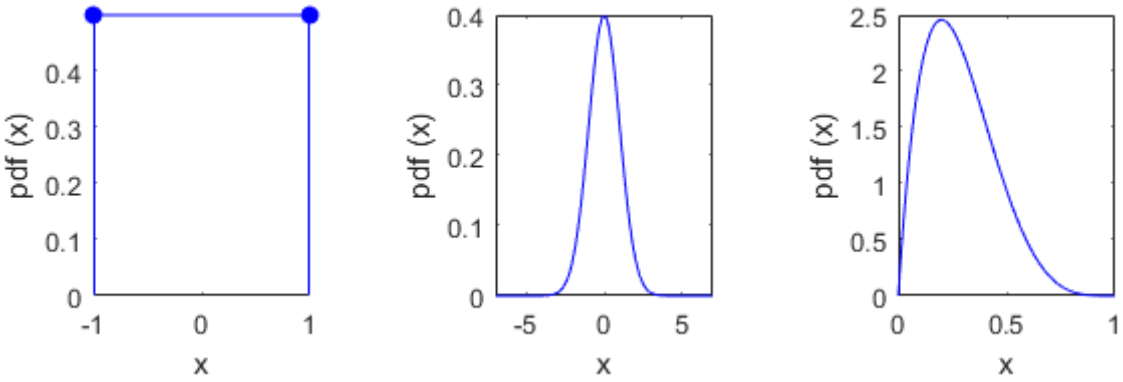

Figure 2.2. The probability density functions (pdf) of a random variable with uniform, standard normal and beta distribution, from left to right, respectively

2.2.Uncertainty propagation (UP)

The first and also the most important step in the stochastic analysis of the output value of interest is the uncertainty propagation (UP) of uncertainties from the input parameters to the output by means of some UP method. Given the model M we seek to represent the output Y as a function of input random variables (Fig. 2.4.). Different methods exist and they can be

classified in several ways. The general classification is into the statistical and non-statistical methods.

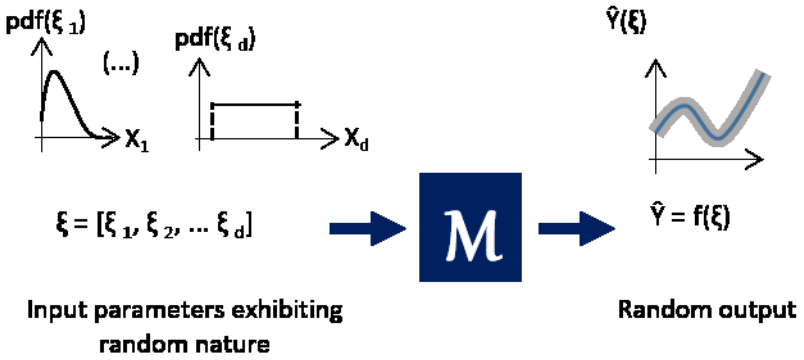

Figure 2.4. The uncertainty propagation (UP) of input uncertainties to the model output

The statistical methods are straightforward to implement as they are all sampling based methods. Their accuracy depends on the sample size which can turn out to be computationally very expensive. However, the sample size does not depend on the stochastic dimensionality of a problem, i.e. the number of random input parameters, which means that the methods do not suffer from the "curse of the dimensionality". Some representative methods in this group are: Monte Carlo (MC) sampling, Latin Hypercube Sampling (LHS), etc.

The aim of non-statistical methods is to avoid the problem of large sample size present at the traditional statistical approaches. Such methods exploit different approaches e.g. the functional approximation theory or novel algorithms for optimization for "smarter" non-statistical sampling, and the combination of them.

The first group of non-statistical methods aims to represent the unknown stochastic solution as a polynomial in the stochastic space of input parameters. Among various techniques available in the literature, two emerged as the most often used approaches in the stochastic CEM. The first one is a spectral discretization based technique, known as the generalized polynomial chaos expansion (gPCE). The gPCE framework implies intrusive approach to dealing with the uncertainties in the input and output parameters which leads to a mandatory change of governing equations [6], [7]. Once the equations are adapted to a stochastic point of view it takes only one run to obtain the desired stochastic output. However, the procedure can be very challenging when the governing equations take complicated forms.

The second non-statistical approach based on the polynomial representation of the output value relies on the high-order stochastic collocation (SC) techniques which are based on

deterministic sampling [6], [8]. Its non-intrusive nature enables the use of previously validated deterministic models as black boxes in stochastic computations, therefore the use of SC is not affected by the complexity or nonlinearity of the original problem [6]. The SC method combines the sampling nature of MC method and the polynomial approximation of the output from the gPCE. Although the total number of samples required for stochastic analysis is lower than in case of MC, the SC method suffers from the "curse of the dimensionality" for large number of input RVs. This problem is alleviated to certain extent by use of high-order methods such as sparse grids and cubature rules. Both gPCE and SC approaches exhibit fast convergence and high accuracy under different conditions which has been reported in many applications. However, it can be stated that gPCE offers the best accuracy in multi-dimensional random spaces and it should always be used when the coupling of gPCE does not involve additional computational cost or when efficient solvers for decoupling the Galerkin system of equations exist [6]. The comparison of the two approaches is documented in [9]-[11]. Both are well established UP methods and their respective variants are still being developed.

In order to outperform the well-established methods such as gPCE and SC, in recent years a different type of non-statistical methods emerged: the methods based on the optimization and pattern classification algorithms [12], [13] and machine learning [14]. In this work a stochastic reduced order model (SROM) method will be outlined.

2.2.1. Monte Carlo method

One of the most commonly used methods for the stochastic simulation of an arbitrary system affected by random variations is Monte Carlo method, or one of its variants. Monte Carlo (MC) is a statistical sampling method popularized by physicists from Los Alamos National Laboratory in the United States in the 1940s. The MC algorithm is robust and relatively simple. Due to its intuitiveness and versatility it is often used for design purposes and also as a reference tool against which other methodologies are compared. The details about the MC based methods are out of the scope of this work, and complete definition with thorough discussion can be found elsewhere, e,g, [15], [16]. Here the MC is considered as a computational algorithm relying on repeated random sampling to obtain statistical information.

The general MC procedure can be outlined as follows:

1. Determine random input parameters and their corresponding distributions.

2. According to distribution of input parameters, generate a set of random samples $\{\boldsymbol{X}^{(k)}\}$ with $k = 1, \ldots N_{MC}$. For $d>1$ each sample is d-dimensional, i.e. $\boldsymbol{X}^{(k)}= [X^{(k)}_1 \ldots X^{(k)}_d]$. It is worth noting that in practical applications a pseudorandom sequences are used [15].
3. The deterministic solver is run repeatedly for each input sample. The output of a model $Y^{(k)}$ is the model realization for the *k-th* input sample: $Y^{(k)} = M(\boldsymbol{X}^{(k)})$. For N_{MC} input samples the MC simulation results in set of output samples $\{Y^{(k)}\}$, $k = 1 \ldots N_{MC}$.
4. The results (N_{MC} outputs of deterministic solver) are collected and analysed in order to obtain the statistical information.

The MC estimators of stochastic moments and probability density function are given as follows. The mean value of the output variable can be estimated by using the following expression:

$$\mu(Y) \approx \hat{\mu}(Y) = \frac{1}{N_{MC}} \sum_{k=1}^{N_{MC}} Y^{(k)} \tag{2.1}$$

Different MC simulations for the same system and with the same number of samples N_{MC} will produce different values of estimated mean value, therefore $\hat{\mu}$ itself is a random variable. The error estimate for the MC method follows directly from the central limit theorem. The set of $\{Y^{(k)}\}$ represents the set of vectors with independent and identically distributed random variables, therefore the distribution function $\hat{\mu}$ converges in the limit of $N_{MC} \rightarrow \infty$, to a Gaussian distribution and the widely adopted concept is that the error convergence rate of MC is inversely proportional to the square root of the number of realizations.

The MC estimator of the variance is given as:

$$\sigma_Y^2 = V(Y) \approx \hat{\sigma}^2 = \frac{1}{N_{MC} - 1} \sum_{k=1}^{N_{MC}} \left(Y^{(k)} - \hat{\mu}\right)^2 \tag{2.2}$$

Beside some specific situations, there is no explicit expression for the variance of the estimator σ_Y^2. Nevertheless, some general qualitative conclusion can be drawn that the convergence rate of the variance estimator is similar to the convergence rate of the mean estimator but its fluctuation will be in general larger.

The probability density function (pdf) of output Y, $f_y(Y)$, is constructed at a discrete set of points $\{Y^{(j)}\}$, $j = 1 \ldots B$, from the samples $\{Y^{(k)}\}$, $k = 1 \ldots N_{MC}$. The points $Y^{(j)}$ are considered

to be equally spaced by $\Delta y=(Y^{(B)} - Y^{(1)}/(B-1)$. The value of the pdf at the point $Y^{(j)}$ can be estimated as:

$$\hat{f}_y\left(Y^{(j)}\right) = \frac{n_j}{N_{MC}\,\Delta y} \tag{2.3}$$

where n_j is the number of samples $Y^{(j)}$ from the interval $[Y^{(j)} - \Delta y/2,\ \ Y^{(j)} + \Delta y/2]$. The pdf of variable Y is approximated by a staircase function, or histogram, were a bin is associated to each point $Y^{(j)}$. The accuracy of the pdf estimator can be improved with large values of B and N_{MC}.

The accuracy of the stochastic moments and the pdf depends directly on the total number of samples N_{MC} and not on the number of random input variables. Thus the method does not suffer from the "curse of the dimensionality". However, the desired accuracy can be accomplished only for a very large N_{MC} which leads to a prohibitive computational burden.

2.3.Sensitivity analysis (SA)

One of the definitions for the sensitivity analysis, adopted in this work as well, is the one describing it as the study of how the uncertainty in the output of a mathematical model or system (numerical or otherwise) can be apportioned to different sources of uncertainty in its inputs [17]. The ideal approach would be to run both uncertainty quantification and sensitivity analysis in the same stochastic framework, usually UQ preceding the SA, thus minimizing the computational burden as much as possible.

There are many SA methods available in literature and the particular choice depends on actual purpose. The extensive study on different SA approaches can be found elsewhere, e.g. in [17]. In this work two approaches will be dealt with: the so-called "one-at-a-time" approach and the approach based on the variance analysis.

2.3.1. "One-at-a-time" (OAT) approach

The idea behind the "one-at-a-time" approach, as the name itself says, is to change the input parameter one at a time while the others are kept at some nominal value. The sensitivity is then measured by monitoring the changes in the output which can be done in different ways, e.g. partial derivatives or linear regression. Within the stochastic framework presented in this work

the sensitivity is measured by monitoring the change in the variance of the output after computing the variance for *d* univariate cases.

Thus, the impact factor of each input parameter is given by the following formula:

$$I_i = V_i(Y)/V(Y) \tag{2.4}$$

where:

$$\boldsymbol{X} = [X_1, X_2, \dots, X_k, \ \dots, X_d] \quad \rightarrow \quad Var(Y|\boldsymbol{X}) = V(Y)$$
$$\mathrm{X} = [X_i] \quad \rightarrow \quad Var(Y|\boldsymbol{X}) = Var(Y|\boldsymbol{X}_i) = V_i(Y)$$

or by simply comparing the variances of the output value for each univariate case.

Although in this way any change observed in the output is unambiguously prescribed to the single variable changed, the approach does not fully explore the input space, since it does not take into account the simultaneous variation of input variables. The OAT approach cannot detect the presence of interactions between input variables.

2.3.2. ANalysis Of VAriance (ANOVA) based method

The ANOVA is an approach originating from the work of Sobol [18] and it is based on variance decomposition within the probabilistic framework. The total variance of a model output is decomposed into terms depending on the input factors and their mutual interactions [17]:

$$V(Y) = \ \sum_k V_k + \ \sum_k \sum_{j>k} V_{kj} + \cdots + V_{12\dots d} \tag{2.5}$$

where *V(Y)* is the output variance when $\boldsymbol{X} = [X_1, \dots, X_d]$, while the other terms are defined as follows:

$$V_k \ = \ V\big(f_k(X_k)\big) \ = \ V_{X_k}\big[E_{X_{\sim k}}(Y|X_k)\big]$$
$$V_{ij} = V\left(f_{ij}(X_i, X_j)\right)$$
$$V\left(f_{ij}(X_i, X_j)\right) = V_{X_i X_j}\left[E_{X_{\sim ij}}(Y|X_i, X_j)\right] - V_{X_i}\left[E_{X_{\sim i}}(Y|X_i)\right] - \ V_{X_i}\left[E_{X_{\sim j}}(Y|X_{ij})\right] \tag{2.6}$$

Normalizing the above expression by total variance *V(Y)* the sensitivity indices are obtained:

$$1 = \sum_k S_k + \sum_k \sum_{j>i} S_{kj} + \cdots + S_{12\ldots d} \tag{2.7}$$

where the first order sensitvity indices measuring the effect of only the k-th random input variable, without any interaction with other RVs, is given by the following expression:

$$S_k = \frac{V_{X_k}\left[E_{X_{\sim k}}(Y|X_k)\right]}{V(Y)}, \quad k = 1, \ldots, d \tag{2.8}$$

The second and high order sensitivity indices, S_{ij} and $S_{12,\ldots d}$ give the infomation about the effect that the interaction of two, ore more random input variables has w.r.t. to the output.

The computational burden may become very prohibitive when all groups of sensitivity indices needs to be computed, therefore, very often only first order sensitivity index is computed. In order to still obtain the information about the potential significant interactions between the varaibles, a total effect sensitivity index is defined as:

$$S_{T_k} = \frac{E_{X_{\sim k}}\left[V_{X_k}(Y|X_{\sim k})\right]}{V(Y)} = 1 - \frac{V_{X_{\sim k}}\left[E_{X_k}(Y|X_{\sim k})\right]}{V(Y)} \tag{2.9}$$

The total effect index measures the contribution to the output variance of X_k, including all variance caused by its interactions, of any order, with any other input variables.

3. Generalized polynomial chaos

The theory of polynomial chaos (PC) has been introduced by Norbert Wiener as a non-sampling based method for uncertainty propagation [19]. In his work, Wiener proposed Hermite type of orthogonal polynomials for basis functions to represent Gaussian random process. Cameron and Martin proved the convergence of such polynomial expansion in L_2 sense for an arbitrary stochastic process with finite second moment, i.e. finite variance [20]. The theory attracted other researchers dealing with the uncertainty quantification problems in different engineering areas, e.g. Ghanem and his co-workers [3].

However, the Hermite polynomials exhibited difficulties in terms of convergence and probability approximations for non-Gaussian problems in some applications. The generalized polynomial chaos (gPC) was introduced by Xiu and Karniadakis in [7] to alleviate these problems. They generalized the results of Cameron & Martin to other continuous and discrete distributions by using orthogonal polynomials from Wiener-Askey scheme presented in the table 3.1.

The gPC theory was further expanded to other types of basis polynomials like piecewise polynomial basis [21], wavelet basis [22] and to a multi-element gPC [23]. Different choice of basis functions exhibited good results depending on the given problem. Furthermore, in [24] Sudret proposes a Sobol-like sensitivity indices directly from the coefficients of the polynomial chaos expansion.

Table 3.1. The Wiener-Askey scheme

Distribution	**pdf**	**Polynomials**	**Weights**	**Support (Γ)**
Uniform	1/2	Legendre	1	$[-1,1]$
Gaussian	$\frac{1}{\sqrt{2\pi}}e^{-\frac{x^2}{2}}$	Hermite	$e^{-\frac{x^2}{2}}$	$[-\infty,\infty]$
Exponential	e^{-x}	Laguerre	e^{-x}	$[0,\infty]$
Beta	$\frac{(1-x)^{\alpha}(1-x)^{\beta}}{B(\alpha,\beta)}$	Jacobi	$(1-x)^{\alpha}(1-x)^{\beta}$	$[-1,1]$

3.1.Polynomial chaos expansion

According to the gPC theory the output variable Y from Fig. 2.4. is approximated by a polynomial expansion [6]:

$$Y(\boldsymbol{\xi}) \approx \hat{Y}(\boldsymbol{\xi}) = \sum_{i=0}^{P} Y_i \varphi_i(\boldsymbol{\xi}) \tag{3.1}$$

where $\{\varphi_i\}$ is a suitable multivariate basis of polynomial functions and Y_i are unknown expansion coefficients to be solved. The expansion is truncated at the order of P.

The polynomial basis functions are orthogonal w.r.t. the inner product in the Hilbert space of d input variables $\boldsymbol{\xi} = [\xi^{(1)}, \xi^{(2)}, ..., \xi^{(d)}]$. More specifically, the set of univariate basis $\{\varphi_i(\xi)\}$ belongs to the space of polynomials orthogonal to the measure $w(\xi)d\xi$ in space Γ. The measure $w(\xi)$ corresponds to a pdf of the variable ξ (table 3.1.). The orthogonality condition for the univariate basis is given as follows [6]:

$$\langle \varphi_i, \varphi_j \rangle = \int_{\Gamma} \varphi_i(\xi)\varphi_j(\xi)w(\xi)d\xi = \alpha_i^2 \delta_{ij} \tag{3.2}$$

where δ_{ij} denotes the Kronecker's delta function and α is a normalization factor that can be determined as:

$$\alpha_i^2 = \langle \varphi_i, \varphi_i \rangle = \int_{\Gamma} \varphi_i^2(\xi)w(\xi)d\xi \tag{3.3}$$

The polynomials are often normalized so that the each factor α_i^2 is set to 1.

Once the maximum degree p of a multivariate basis is chosen it is possible to obtain its elements as a product of univariate polynomials in each direction (dimension) $\xi^{(k)}$, $k = 1, ..., d$:

$$\varphi_{\boldsymbol{i}}(\boldsymbol{\xi}) = \prod_{k=1}^{d} \varphi_{\boldsymbol{i}}^{(k)}\left(\xi^{(k)}\right), \qquad \sum_{k=1}^{d} m_k \leq p \tag{3.4}$$

where $\varphi_{\boldsymbol{i}}(\boldsymbol{\xi})$ is a multivariate basis of degree p. The polynom $\varphi_{\boldsymbol{i}}^{(k)}(\xi)$ is a univariate basis in the k-th dimension whose degree is denoted with m_k, thus the multidimensional index is given as $\boldsymbol{i} = [m_1, m_2, ..., m_d]$. The set $\{\varphi_{\boldsymbol{i}}(\boldsymbol{\xi})\}$ defines the space of the d-variate orthogonal polynomials whose total degree is at most p. The table 3.2. exhibits the series of multivariate functions for $d = 2$ and p chosen to be at most 3.

Table 3.2. The set of bivariate (d=2, $\boldsymbol{\xi} = [\xi^{(1)}, \xi^{(2)}]$) basis functions for the maximum degree of multivariate polynomial p = 3

$\boldsymbol{i = [m_1, m_2]}$	i	p	**Multivariate polynomal:** $\boldsymbol{\varphi_i(\xi)}$
[0, 0]	1	0	$\varphi_0(\xi^{(1)}) \cdot \varphi_0(\xi^{(2)})$
[1, 0]	2	1	$\varphi_1(\xi^{(1)}) \cdot \varphi_0(\xi^{(2)})$
[0, 1]	3		$\varphi_0(\xi^{(1)}) \cdot \varphi_1(\xi^{(2)})$
[2, 0]	4	2	$\varphi_2(\xi^{(1)}) \cdot \varphi_0(\xi^{(2)})$
[1, 1]	5		$\varphi_1(\xi^{(1)}) \cdot \varphi_1(\xi^{(2)})$
[0, 2]	6		$\varphi_0(\xi^{(1)}) \cdot \varphi_2(\xi^{(2)})$
[3, 0]	7	3	$\varphi_3(\xi^{(1)}) \cdot \varphi_1(\xi^{(2)})$
[2, 1]	8		$\varphi_2(\xi^{(1)}) \cdot \varphi_1(\xi^{(2)})$
[1, 2]	9		$\varphi_1(\xi^{(1)}) \cdot \varphi_2(\xi^{(2)})$
[0, 3]	10		$\varphi_0(\xi^{(1)}) \cdot \varphi_3(\xi^{(2)})$

The expansion of the output Y given in (3.1) is truncated at the value P. In practice the value of P depends on the total polynomial degree p and number of input random variables d [6]:

$$(P+1) = \binom{d+p}{p} = \frac{(p+d)!}{p!\,d!} \tag{3.5}$$

The orthogonality property from eq. (3.2.) extends to the multivariate basis:

$$\begin{aligned} \langle \varphi_i, \varphi_j \rangle &= \int_\Gamma \varphi_i(\boldsymbol{\xi}) \varphi_j(\boldsymbol{\xi}) w(\boldsymbol{\xi}) d\boldsymbol{\xi} \\ &= \prod_{k=1}^{d} \int_\Gamma \varphi_{\boldsymbol{i}}^{(k)}(\xi^{(k)}) \cdot \varphi_{\boldsymbol{j}}^{(k)}(\xi^{(k)}) w(\xi^{(k)})\, d\xi^{(k)} = \prod_{k=1}^{d} \langle \varphi_i^{(k)}, \varphi_j^{(k)} \rangle \end{aligned} \tag{3.6}$$

The former expression differs from zero only if $i^{(k)} = j^{(k)}$, $k = 1, \ldots, d$ which happens when the two multivariate polynomials are identical.

For the purpose of illustration, the output Y will be approximated by using Hermite polynomial basis. The Hermite polynomials up to degree $p = 3$ are given as [6]:

$$H_0(\xi) = 1 \;\; H_1(\xi) = \xi \;\; H_2(\xi) = \frac{\xi^2 - 1}{\sqrt{2}} \;\; H_3(\xi) = \frac{\xi^3 - 3\xi}{\sqrt{6}} \tag{3.7}$$

where polynomial basis φ_i is denoted as H_i in the case of Hermitian basis type.

Suppose we have a bivariate case, $d = 2$. The truncation based on $d = 2$ and $p = 3$ leads to $P = 9$. Thus the polynomial approximation for the output $Y(\xi^{(1)}, \xi^{(2)})$ is as follows:

$$\hat{Y}\left(\xi^{(1)}, \xi^{(2)}\right) = Y_0 + Y_1 \cdot \xi^{(1)} + Y_2 \cdot \xi^{(2)} + Y_3 \cdot \frac{\left(\xi^{(1)}\right)^2 - 1}{\sqrt{2}} + Y_4 \cdot \xi^{(1)} \cdot \xi^{(2)} + Y_5 \cdot \frac{\left(\xi^{(2)}\right)^2 - 1}{\sqrt{2}} + Y_6 \cdot \frac{\left(\xi^{(1)}\right)^3 - 3\xi^{(1)}}{\sqrt{6}} + Y_7 \cdot \frac{\left(\xi^{(1)}\right)^3 - 3\xi^{(2)}}{\sqrt{6}} + Y_8 \cdot \frac{\left(\xi^{(2)}\right)^3 - 3\xi^{(1)}}{\sqrt{6}} + Y_9 \cdot \frac{\left(\xi^{(2)}\right)^3 - 3\xi^{(2)}}{\sqrt{6}} \tag{3.8}$$

Given that the polynomials from Wiener-Askey scheme (table 3.1.) form a complete basis in the Hilbert space determined by the corresponding support Γ, the expansion is the best approximation in the linear polynomial space spanned by $\{\varphi_i\}$. It converges in the L_2 sense and with the increase of p [6].

3.2.Computation of the coefficients

The coefficients Y_i in the expansion given by the expression (3.1.) can be computed by means of orthogonal projection onto the polynomial basis as follows:

$$Y_i = \frac{\langle Y, \varphi_i \rangle}{\langle \varphi_i, \varphi_i \rangle} = \frac{\int_\Gamma Y(\boldsymbol{\xi}) \varphi_i(\boldsymbol{\xi}) w(\boldsymbol{\xi}) d\boldsymbol{\xi}}{\alpha_i^2} \tag{3.5}$$

The integral in (3.5) contains the unknown quantity of interest Y, hence it is computed numerically by means of either collocation or Galerkin methods [6]. The Galerkin approach, also known as stochastic Galerkin method (SG) is often used in case of relatively simple governing equations [6]. The collocation based approaches for computing the expansion coefficients are used when the governining equations take more complicated forms. The combination of the gPC and collocation approaches is known as the pseudospectral approach [25].

3.3.Statistical information

The polynomial expansion (3.1.) is an analytical relationship between the output Y and the random input parameters $\boldsymbol{\xi} = [\xi^{(1)}, \xi^{(2)}, \ldots, \xi^{(d)}]$ thus providing a sort of a surrogate for the original deterministic model. With P large enough the polynomial representation is quite accurate and the statistical information can be obtained. The property of orthogonality in eq.

(3.2) yields that every polynomial is orthogonal to the one with the degree 0, i.e. $\varphi_0(\xi) = 1$. Consequently, the expectation of every other polynomial whose degree $m_k \neq 0$ is zero. Thus, by using the property of orthogonality and following the definitions from the statistics for the stochastic moments, the mean and the variance are given as follows [6].

- The stochastic mean or expected value:

$$E\{Y(\boldsymbol{\xi})\} \approx E\{\hat{Y}(\boldsymbol{\xi})\} = \int_{\Gamma} \hat{Y}(\boldsymbol{\xi}) w(\boldsymbol{\xi}) d\boldsymbol{\xi} = \sum_{i=0}^{P} Y_i \int_{\Gamma} \varphi_i(\boldsymbol{\xi}) w(\boldsymbol{\xi}) d\boldsymbol{\xi} \equiv \sum_{i=0}^{P} Y_i \frac{1}{\alpha_0} \langle \varphi_i, \varphi_0 \rangle = Y_0 \alpha_0 \tag{3.6}$$

- The variance:

$$\begin{aligned} Var\{Y(\boldsymbol{\xi})\} &\approx Var\{\hat{Y}(\boldsymbol{\xi})\} = \int_{\Gamma} \hat{Y}^2(\boldsymbol{\xi}) w(\boldsymbol{\xi}) d\boldsymbol{\xi} - E\{\hat{Y}(\boldsymbol{\xi})\}^2 = \\ &\sum_{i=0}^{P} \sum_{j=0}^{P} Y_i Y_j \int_{\Gamma} \varphi_i(\boldsymbol{\xi}) \varphi_j(\boldsymbol{\xi}) w(\boldsymbol{\xi}) d\boldsymbol{\xi} - Y_0^2 \alpha_0^2 \\ = \sum_{i=0}^{P} \sum_{j=0}^{P} Y_i Y_j \langle \varphi_i, \varphi_j \rangle - Y_0^2 \alpha_0^2 &= \sum_{i=0}^{P} Y_i^2 \alpha_i^2 - Y_0^2 \alpha_0^2 = \sum_{i=1}^{P} Y_i^2 \alpha_i^2 \end{aligned} \tag{3.7}$$

- The calculation of pdf:

In case of the calculation of pdf the polynomial expansion given by (3.1) can be treated by Monte Carlo sampling as described in 2.2.1.

3.4.Application example

For the sake of completeness the main PCE properties will be illustrated through a very simple example. We choose a Gaussian random variable X with mean $\mu = 5$ and standard deviation $\sigma = 0.7$, i.e. $X \sim N(5,0.7)$. Furthermore, we define the output Y as a random variable depending on the X such that:

$$Y = M(X) = 2X^2 - 3X - 4 \tag{3.8}$$

Then, the random variable X is expressed in terms of the normalized random variable $\xi \sim N(0,1)$ as follows:

$$X = 5 + 0.7\xi \tag{3.9}$$

By inserting (3.8.) into (3.7.) the output Y can be expressed as the following polynomial:

$$Y(\xi) = 0.98\xi^2 + 11.9\xi + 31 \tag{3.10}$$

Moreover, the above expression may be written as a second-order Hermite expansion:

$$Y(\xi) = 31.98 + 11.9\xi + 1.39 \cdot \left(\frac{\xi^2 - 1}{\sqrt{2}}\right)$$
$$Y(\xi) = 31.98 \cdot H_0(\xi) + 11.9H_1(\xi) + 1.39H_2(\xi) \quad (3.11)$$

According to (3.6.) and (3.7.) the results for the mean and variance are: $E\{Y\} = 0! \cdot 31.98$ and $Var(Y) = 1! \cdot 11.9^2 + 2! \cdot 1.39^2 = 143.54$, respectively. The MCM results for the mean and the variance with $N_{MC} = 10.000.000$ samples are $\mu_{MC} = 31.98$ and $\sigma^2_{MC} = 143.48$.

4. Stochastic collocation method

Similarly to the gPC theory, the fundamental principle of stochastic collocation (SC) lies in the polynomial approximation of the considered output Y for d random input parameters [6]. The expansion coefficients for the stochastic collocation are actually the deterministic outputs of the considered model, calculated at N_{sc} predetermined input points also called the collocation points. However, not all classical sampling methods are automatically labelled as stochastic collocation. Instead, the term "stochastic collocation" is reserved for the type of collocation methods that result in a strong convergence, e.g. mean-square convergence, to the true solution [26]. This is typically achieved by utilizing the classical multivariate approximation theory to strategically locate the collocation nodes in order to construct a polynomial approximation to the solution.

Hence, the fundamental principle of the SC method lies in the polynomial approximation of the considered output Y over the d dimensional input stochastic space in which N_{sc} samples are previously selected [26]:

$$\hat{Y}(\boldsymbol{\xi}) = \sum_{i=1}^{N} L_i(\boldsymbol{\xi}) \cdot Y^{(i)} \tag{4.1}$$

where $L_i(\boldsymbol{\xi})$ is basis function and $Y^{(i)}$ is the output realization for the i-th input point $\boldsymbol{\xi}^{(i)}$. Note that the transformation of the vector of random input variables to a vector of standardized random input variables is assumed ($\boldsymbol{X}^{(i)}=[X_1^{(i)}, ..., X_d^{(i)}]$ into $\boldsymbol{\xi}^{(i)}=[\xi_1^{(i)}, ..., \xi_d^{(i)}]$).

There are two issues to be considered: how to construct the basis functions $L_i(\boldsymbol{\xi})$ and how to choose interpolation points $Y^{(i)} = M[\boldsymbol{X}^{(i)}]$. Again, different approaches exist to answer these challenges. The basis functions may be of Lagrange type [8], wavelet basis [27] or piecewise constant [28] while the choice of the collocation points may follow different quadrature [8] and cubature rules [29].

Furthermore, some effort has been done regarding the coupling of the uncertainty quantification and sensitivity analysis in the same stochastic collocation framework. Buzzad and Xiu exploited the nature of sparse grid interpolation and cubature methods of Smolyak together with combinatorial analysis to give a computationally efficient method for computing the global sensitivity values of Sobol' [30]. Furthermore, Tang and Iaccarino showed the accuracy and efficiency of Sobol like indices computed by using the SC method in [31]. SC methodology has also been used for inverse problems under the Bayesian approach. The aim

of inverse problems is to reduce the uncertainty of the input parameters in order to make predictions, and even to devise control strategies based on the predictions [32]. The Bayesian inference in the SC framework has been reported in [33]- [35].

4.1.Computation of stochastic moments

To address the questions pertaining to the choice of basis function and collocation points, it is useful to firstly recall the definitions of stochastic moments. According to the statistics' theory the first two moments are defined as follows:

$$\mu\big(Y(\boldsymbol{\xi})\big) = \int_{\Gamma} Y(\boldsymbol{\xi}) p(\boldsymbol{\xi}) d\boldsymbol{\xi} \tag{4.2.a}$$

$$\begin{aligned} Var(Y) &= \mathrm{E}[(Y - E[Y])^2] = E\big[Y^2 - 2YE[Y] + E[Y]^2\big] \\ &= \mathrm{E}[Y^2] - 2E[Y]E[Y] + E[Y]^2 = E[Y^2] - E[Y]^2 \end{aligned} \tag{4.2.b}$$

$$Var\big(Y(\boldsymbol{\xi})\big) = \int_{\Gamma} \Big(Y(\boldsymbol{\xi}) - \mu\big(Y(\boldsymbol{\xi})\big)\Big)^2 p(\boldsymbol{\xi}) d\boldsymbol{\xi}$$

where $p(\boldsymbol{\xi})$ is the joint probability density function defined as follows:

$$p(\boldsymbol{\xi}) = \prod_{k=1}^{d} p(\xi_k) \tag{4.3}$$

Inserting (4.1.) into (4.2) it follows:

$$\mu\big(Y(\boldsymbol{\xi})\big) \approx \int_{\Gamma} \sum_{i=1}^{N} L_i(\boldsymbol{\xi}) \cdot Y^{(i)} p(\boldsymbol{\xi}) d\boldsymbol{\xi} = \sum_{i=1}^{N} Y^{(i)} \int_{\Gamma} L_i(\boldsymbol{\xi}) \cdot p(\boldsymbol{\xi}) d\boldsymbol{\xi} \tag{4.4.a}$$

and

$$\begin{aligned} Var\big(Y(\boldsymbol{\xi})\big) &= \int_{\Gamma} \Big(Y(\boldsymbol{\xi}) - \mu\big(Y(\boldsymbol{\xi})\big)\Big)^2 p(\boldsymbol{\xi}) d\boldsymbol{\xi} \\ Var\big(Y(\boldsymbol{\xi})\big) &= \sum_{i=1}^{N} \big(Y^{(i)}\big)^2 \int_{\Gamma} L_i(\boldsymbol{\xi}) \cdot p(\boldsymbol{\xi}) d\boldsymbol{\xi} - \mu\left(\hat{Y}(\boldsymbol{\xi})\right)^2 \end{aligned} \tag{4.4.b}$$

Given that the basis functions $L_i(\boldsymbol{\xi})$ and the joint pdf $p(\boldsymbol{\xi})$ are known, the integral over the space Γ can be precomputed and its value is called the weight w_i:

$$w_i = \int_{\Gamma} L_i(\boldsymbol{\xi}) p(\boldsymbol{\xi}) d\boldsymbol{\xi} \tag{4.6}$$

Consequently, the stochastic moments can be expressed in a very simple form. The expressions for the first four stochastic moments are given in table 4.1. The higher orders of stochastic moments are computed accordingly [26].

Table 4.1. The expressions for the first four stochastic moments

Stochastic moment		**Expression:**
1	mean	$\mu\big(Y(\boldsymbol{\xi})\big) \approx \sum_{i=1}^{N} Y^{(i)} w_i$
2	variance	$\sigma_Y^2 = Var(Y) \approx \sum_{i=1}^{N} \big(Y^{(i)}\big)^2 w_i - \mu^2$
3	skewness	$skew(Y) \approx \dfrac{\sum_{i=1}^{N} \big(Y^{(i)}\big)^3 w_i - 3\mu\sigma_Y^2 - \mu^3}{\sigma_Y^3}$
4	kurtosis	$kurt(Y) \approx \dfrac{\sum_{i=1}^{N} \big(Y^{(i)}\big)^4 w_i - 4\mu \cdot skew \cdot \sigma_Y^3 - 6\mu^2 \cdot \sigma_Y^2 - \mu^4}{\sigma_Y^4}$

4.2.Interpolation approaches

The most popular approach to choosing the basis function is by following the well-developed and extensive classical theory of univariate Lagrange polynomial interpolation [26]. Hence, for the univariate case, i.e. $d = 1$ & $\boldsymbol{\xi}^{(i)}=[\ \xi_1^{(i)}]$ and total of m_k collocation points in the k-th dimension the Lagrange basis function is given as:

$$l_i(\xi_{\boldsymbol{k}}) = \prod_{j=0,\ j\neq i}^{m_k} \frac{\xi_{\boldsymbol{k}} - \xi_{\boldsymbol{k}}^{(j)}}{\xi_k^{(i)} - \xi_{\boldsymbol{k}}^{(j)}} \quad i = 1, \dots, m_k \tag{4.7}$$

with the property

$$l_i\big(\xi_{\boldsymbol{j}}\big) = \delta_{ij} \tag{4.8}$$

where δ_{ij} denotes Kronecker symbol.

The alternative approach is to use piecewise linear functions defined as follows:

$$l(\xi_k)_j^{(u)} = \begin{cases} 1 - \left(m_k^{(u)} - 1\right) \cdot \left|\xi_k - \xi_k^{(u)}{}_j\right|, & if\ \left|\xi_k - \xi_k^{(u)}{}_j\right| < \frac{1}{m_k^{(u)} - 1} \\ 0 & otherwise \end{cases} \tag{4.9}$$

The total number of m_k collocation points in the k-th dimension is defined as:

$$m_k^{(u)} = \begin{cases} 1, & for\ u = 1 \\ 2^{u-1} + 1, & for\ u > 1 \end{cases} \tag{4.10}$$

where u is the level of supporting point.

Lagrange polynomials have the character of locally global basis functions, while piecewise linear basis functions are used when it is important to capture the discontinuous issues in stochastic solutions. Since the manipulation of Lagrange or other type of basis function may be a cumbersome procedure, a pseudo-spectral collocation approach is proposed in [25] and it is considered as a part of gPC theory described briefly in section 3.

4.3.Collocation points selection

The choice of the collocation points is essential part of any collocation based method. The aim of stochastic collocation method is to approximate the integral in the equation (4.6.) as accurate as possible:

$$w_i = \int_{\Gamma} L_i(\boldsymbol{\xi}) p(\boldsymbol{\xi}) d\boldsymbol{\xi}$$

The weights w_i are computed numerically. However, as long as the stochastic dimension is equal to 1 ($d = 1$) the points selection is straightforward. There are numerous numerical studies proposing wide range of quadrature rules to deal with the 1-dimensional integral evaluation and the optimal choice is Gauss quadrature [6]. Depending on the pdf of the input RV one can choose between different Gauss quadrature rules, e.g. Gauss-Hermite, Gauss-Legendre or Gauss-Jacobi for variables with normal, uniform or beta distributions, respectively [6]. It is worth noting that this corresponds to the Wiener-Askey scheme (table 3.1).

E.g. for the variable $X = 5$, uniformly distributed in the interval $U = [2, 8]$, the selection of collocation points follows Gauss-Legendre quadrature rule which belong to interval [-1, 1]. In order to estimate the stochastic moments given by expressions in table 3.1., the mathematical model will be run N times, where N corresponds to the number of collocation points. The accuracy is increased with the selected number of collocation points needed for the computation of the integral (4.6). The Gauss-Legendre quadrature points are given in table 4.2. for odd values of N along with the corresponding collocation points of variable X and their respective weights. The basis functions used in this example are of Lagrange type.

Table 4.2. Collocation points for random variable uniformly distributed in range [2, 8]

N	ξ = [-1, 1]	X = [2, 8]	$w_i = \int_\Gamma L_i(\xi)p(\xi)d\xi$
3	-0.7746	2.6762	0.2778
	0	5.0000	0.4444
	0.7746	7.3238	0.2778
5	-0.9062	2.2815	0.1185
	-0.5385	3.3846	0.2393
	0	5.0000	0.2844
	0.5385	6.6154	0.2393
	0.9062	7.7185	0.1185

It is worth noting that the computation of weights does not depend on the boundary values of variable *X*, therefore, they can be precomputed and stored for further use.

Other integration rules may be used as well. Very often instead of Gauss quadrature a Clenshaw-Curtis quadrature rule is used, especially when sparse grid multi-variate interpolation is employed [26] which will be further discussed in the following subsections. Additionally, it is a practice to use equidistant points when the interpolation is done by using the piecewise linear basis funcitons.

The real challenge, however, is a numerical computation of multi-dimensional integral for $d > 1$, especially for $d >> 1$. For extremely large dimensions in realistic scenarios the Monte Carlo method and its variants are still the only applicable approaches. However, if the dimension is not too large there are quicker approaches which are also used in the framework of SC method.

4.3.1. Tensor product

The most natural approach to multi-dimensional integration is the tensor product of 1-dimensional quadrature rules which leads to relatively simple generalization of integration properties from 1-dimensional to *d*-dimensional case [26]. The idea of tensor product has been introduced in [8], [36] and its errors are analysed in [37].

The multi-dimensional integral (4.6.) is thus given as:

$$w_i = \int_{\Gamma_1} l\left(\xi_1^{(i)}\right)p(\xi_1)d\xi \cdot \int_{\Gamma_2} l\left(\xi_2^{(i)}\right)p(\xi_2)\xi \cdot \ \ldots \ \cdot \int_{\Gamma_d} l\left(\xi_d^{(i)}\right)p(\xi_d)d\xi \qquad (4.11)$$

$$w_i = w_{1_{(j)}}^{(i)} \cdot w_{2_{(j)}}^{(i)} \cdot \ \dots \ \cdot w_{d_{(j)}}^{(i)} \qquad i = 1, \dots, N_{SC}$$

The multivariate basis functions $L_i(\boldsymbol{\xi})$ from eq. (4.1.) are also formed by means of a tensor product of a univariate basis functions in each dimension:

$$L_i(\boldsymbol{\xi}) = l\left(\xi_1^{(i)}\right) \otimes l\left(\xi_2^{(i)}\right) \otimes \dots \otimes l\left(\xi_d^{(i)}\right) \tag{4.12}$$

The total number of simulation points is thus:

$$N_{SC} = \prod_{k=1}^{d} m_k \tag{4.13}$$

In most of the applications the number of collocation points in each dimension is equal, thus $N_{SC} = m_k \hat{} d$. Obviously, the number of simulation points grows exponentially with the number of input RVs, therefore the tensor product is mostly used at lower dimensions. The generally accepted limitation is $d \leq 5$ [26].

4.3.2. Sparse grids

The idea behind the sparse grids is to alleviate the problem of a "curse of dimensionality" present in the tensor product by using a sparse instead of a tensorized grid of points. The approach was first proposed by Smolyak in [38] and it has been widely used and improved ever since in the context of multivariate integration and interpolation [39], [40]. The sparse grids were introduced to stochastic collocation framework in [26].

The sparse grid represents the subset of the full tensor product grid. The basic idea behind the sparse grid is an optimal linear approximation of the low level tensor products such that an integration property for $d = 1$ is preserved as much as possible for $d > 1$ [26]. Consequently, only those products with the relatively small number of points are used thus reducing the total number of simulation points. Lots of prominent researchers investigated different algorithms for sparse grid construction and perhaps the most famous works are those of Griebel and Zenger [41], [42].

The classical sparse-grid approach applied to the construction of multi-variate basis function $L_i(\boldsymbol{\xi})$ can be expressed in the following way [26]:

$$L_i(\boldsymbol{\xi}) = \sum_{q+1 \leq |\vec{h}| \leq q+\boldsymbol{d}} (-1)^{q+\boldsymbol{d}-|\vec{h}|} \cdot \binom{\boldsymbol{d}-1}{q+\boldsymbol{d}-|\vec{h}|} \cdot \left(l\left(\xi_{\boldsymbol{1}}^{(i)}, h_{\boldsymbol{1}}\right) \otimes \dots \otimes l\left(\xi_d^{(i)}, h_{\boldsymbol{d}}\right) \right) \tag{4.14.}$$

where q is a sparseness parameter or the sparseness level and h denotes the depth coordinate for each dimension: k= 1, …, d. The vector $|\mathbf{h}| = h_1 + h_2 + \ldots h_d$ lists the levels of the rules used by each component. The algorithms for a sparse grid construction may be found in [41].

It is worth noting that there is no mandatory choice of the one-dimensional quadrature rules used in the sparse grid algorithm. However, in order to reuse the collocation points from lower levels h in the higher levels as well, it is a good practice to use those quadrature rules that result in a set of nested points. As an example, Fig. 4.3. illustrates the sequence of Gauss-Hermite collocation points and the sequence of Clenshaw-Curtis points computed as the extrema of the Chebyshev polynomials. As it is obvious from the figure, at the individual level h number of Gauss rule results in less number of points w.r.t. Clenshaw-Curtis rule. Nevertheless, due to the nesting property of Clenshaw-Curtis set of points, the total number of 17 points is less than total of 21 Gauss points.

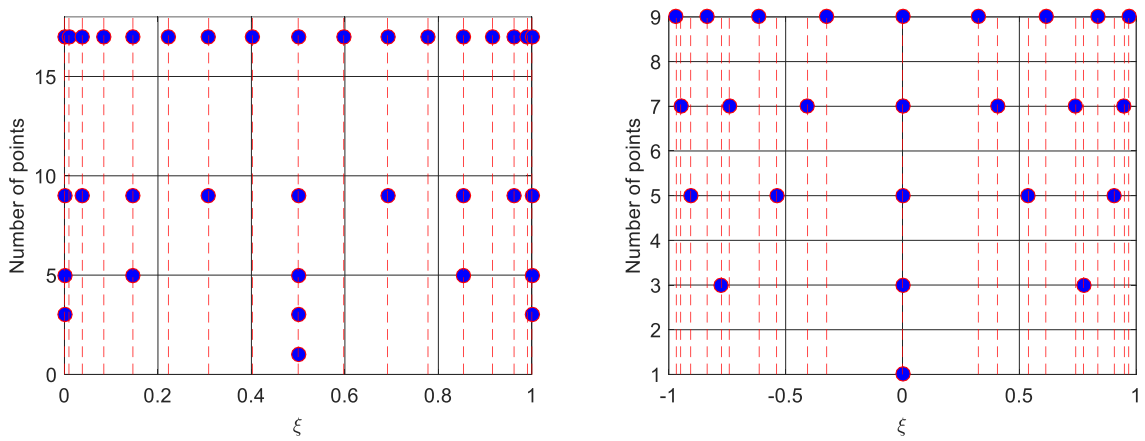

Figure 4.3. The Clenshaw-Curtis (left) vs. Gauss-Hermite (right) sequence of points for 5 levels of interpolation

For the sake of completeness a simple example with $d = 3$ random input variables uniformly distributed in the interval [-1, 1] is depicted in Fig. 4.4. The grids of points are presented for MC simulation and both for tensor and sparse grid of points. The sparseness level is set to q = 2 and Clenshaw-Curtis quadrature was used, while Gauss-Legendre quadrature was used with the tensor product. The total number of points for the different techniques is N_{MC} = 1000, $N_{SC\text{-}SG}$ = 69 and N_{SC} = 343, respectively.

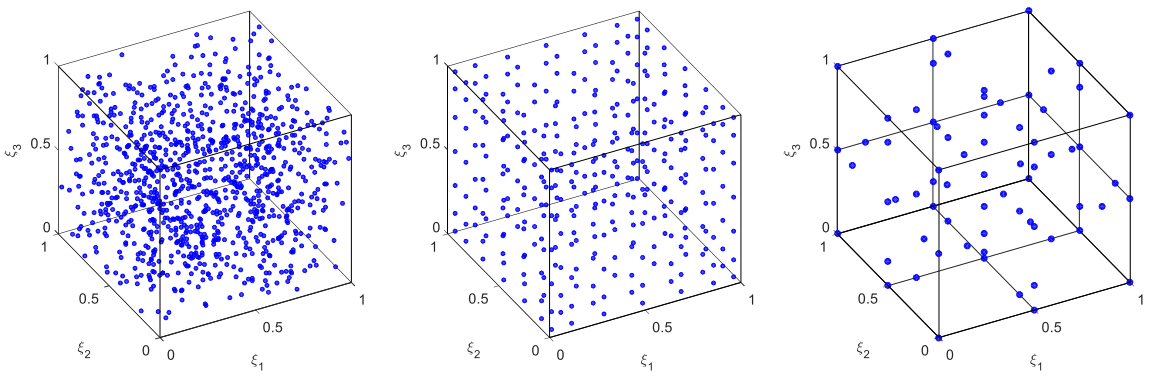

Figure 4.4. The 3-dimensional grid of points for MC, SC-tensor grid and SC-sparse grid techniques (left to right)

The dependence of the total number of simulation points of the sparse grid products on the dimension is much weaker than in case of tensor product with the reduction from $N_{SC} = m_k\text{^}d$ to approximately $N_{SC\text{-}SG} = (2*m_k)\text{^}d / d!$ simulation points. The sparse grid approximation is accurate for d > 5. Some of the first sparse grid SC computations in [26] went to 50-dimensional stochastic space.

4.3.3. Stroud's cubature rules

The integration rules for the evaluation of multidimensional integrals, also known as cubature rules, are a part of an active research. Cools has published a collection of available cubature formulas for the approximation of multivariate integrals over some standard regions in [43]. As it is the case for every rule for numerical integration, the idea is to represent the multidimensional integral as a sum of products of weights ω_i and the function evaluations at a carefully chosen points $\xi^{(i)}$:

$$\int_{[-1,1]^d} f(\boldsymbol{\xi}) d\boldsymbol{\xi} = \sum_{i=1}^{M} \omega_i f\left(\boldsymbol{\xi}^{(i)}\right) \tag{4.16}$$

where $[-1,1]^d$ is the hypercube space.

A large collection of cubature rules can be a good option for SC technique and the most used ones are the Stroud's cubatures [26]. Stroud proposed two set of cubature points, one accurate for multiple integrals of polynomials of degree 2 and the other for polynomials of degree 3, the Stroud-2 and Stroud-3 formulas, respectively [44].

The Stroud-2 formula is given as follows:

$$\xi_{2r-1}^{(i)} = \sqrt{\frac{2}{3}}\cos\left(\frac{2r(i-1)\pi}{d+1}\right) \;\&\; \xi_{2r}^{(i)} = \sqrt{\frac{2}{3}}\sin\left(\frac{2r(i-1)\pi}{d+1}\right), \;\; \omega_i = \frac{1}{d+1}$$
$$r = 1, 2, \ldots, floor\left(\frac{d}{2}\right) \tag{4.17}$$

provided that *d* is an even number. If number *d* is odd, the location of the i-th node for the d-th dimension is given by the following expression:

$$\xi_d^{(i)} = \frac{(-1)^{i-1}}{\sqrt{3}} \tag{4.18}$$

while the formula for weights ω_i remains the same.

The Stroud-3 formula is defined with:

$$\xi_{2r-1}^{(i)} = \sqrt{\frac{2}{3}}\cos\left(\frac{(2r-1)i\pi}{d}\right) \;\&\; \xi_{2r}^{(i)} = \sqrt{\frac{2}{3}}\sin\left(\frac{(2r-1)i\pi}{d+1}\right), \;\; \omega_i = \frac{1}{2d}$$
$$r = 1, 2, \ldots, floor\left(\frac{d}{2}\right) \tag{4.19}$$

again with the additional expression for the i-th node along the last dimension:

$$\xi_d^{(i)} = \frac{(-1)^{i}}{\sqrt{3}} \tag{4.20}$$

The total number of collocation points given by Stroud-2 rule is *M = (d + 1)* while in case of Stroud-3 rule *M = 2*d*. The number *M* is fixed, it depends only on the dimensionality of a stochastic model and it is a minimal number of points necessary for the desired integration accuracy of a polynomials with the corresponding degree. It is worth noting that Stroud rules present a good choice when the demand on accuracy is not very strict in case of high-dimensional stochastic spaces (d >> 1) [26].

5. Stochastic reduced order model

In the area of stochastic computations the never ending aspiration is to develop a model that has a computational cost as low as possible at the same time preserving the accuracy of results. In this spirit, much effort has been invested in the so called reduced models. In particular, the aim is to develop a stochastic model that can deal with the existing deterministic systems in a non-intrusive manner with as few sampling as possible. One of the new techniques that has been proposed is the stochastic reduced order model (SROM).

Stochastic reduced order model - SROM, is a new technique of solving stochastic problems that can be described in the following way: SROM is a reduced representation of the input variable constructed with the goal to preserve its statistical properties [12]. A brief overview of the progress in SROM development is presented in this section. The main idea behind the SROM is introduced, some proposed algorithms are outlined and basic examples are provided.

5.1.Generalities on SROM

A SROM of a random variable $\boldsymbol{X}$ is a simple vector$\tilde{X}$ with finite number of samples that approximates the variable in such a way that $\boldsymbol{X}$ and $\tilde{X}$ have similar statistical properties. The SROM is completely defined with its samples and the assigned probability to each sample. This property makes it different from a Monte Carlo approach in which a large set of equally likely samples is generated [12].

SROM is defined by:

$$\tilde{X}_{SROM} = \tilde{X} = \{(\tilde{x}_k, p_k)\}, \qquad 1 \leq k \leq m \tag{5.1}$$

with constraints:

$$\sum_{k=1}^{m} p_k = 1, \qquad p_k \geq 0\,, \quad 1 \leq k \leq m \tag{5.2}$$

where $\tilde{x}_k$ are sample values, and p_k is a probability assigned to each value. The cardinal number m is determined apriori and it represents the size of a SROM. Its value depends on the computational requirements for a particular application.

As it is reported in [45] any m samples of variable X along with prescribed probabilities that satisfy the constraints make a SROM for X. Still, these representations of X are most likely unsatisfactory since one needs to make sure that the probability laws of X and $\tilde{X}$ are as similar

as possible. The general way to assure the optimal representation is to minimize the discrepancy between statistical properties of X and $\tilde{X}$ by solving the optimization problem. This is the core of SROM construction and it is also the only overhead to deal with when applying SROM to a problem. Several optimization techniques have been proposed in various papers and they are briefly outlined in the following subsection.

Although various metrics can be used to measure the discrepancy between X and $\tilde{X}$, the most common way is to account for the difference between their marginal distributions, marginal moments up to order six and correlation function. All of this is possible if the statistical properties of X are well known. On the contrary, if this is not the case the alternative optimization problem must be formulated [12].

Hence, let's assume that X is a d dimensional random variable whose statistical properties are completely known: $X=[X_1, X_2, \ldots, X_d]$. By statistical properties the following is assumed: marginal distribution, moments of order r, and correlation matrix:

$$F_i(\vartheta) = P(X_i \leq \vartheta) \tag{5.3}$$

$$\mu_i(r) = E(X_i^r) \tag{5.4}$$

$$\boldsymbol{r} = E[\boldsymbol{X}\boldsymbol{X}^{\boldsymbol{T}}] \tag{5.5}$$

where $i = 1, \ldots, d$.

The marginal distribution (cumulative density function, cdf), moments of order r, and correlation matrix are defined for SROM $\tilde{X}$ in the following way:

$$\tilde{F}_i(\vartheta) = P\left(\tilde{X}_i \leq \vartheta\right) = \sum_{k=1}^{m} p_k \boldsymbol{I}\left(\tilde{x}_{k,i} \leq \vartheta\right) \tag{5.6}$$

$$\tilde{\mu}_i(r) = E\left(\tilde{X}_i^r\right) = \sum_{k=1}^{m} p_k \left(\tilde{x}_{k,i}\right)^r \tag{5.7}$$

$$\tilde{\boldsymbol{r}}_{i,j} = E\left[\tilde{\boldsymbol{X}}_i \tilde{\boldsymbol{X}}_j\right] = \sum_{k=1}^{m} p_k \tilde{x}_{k,i} \tilde{x}_{k,j} \tag{5.8}$$

where $i = 1, \ldots, d$ and $I(A) = 1$ if A true, 0 if A false as an indicator function.

The optimization function that minimizes the discrepancy between statistical properties is defined as:

$$f = \sum_{u=1}^{3} \alpha_u \, e_u \tag{5.9}$$

where e_u are measures for discrepancies between the marginal distributions, moments up to order $\tilde{r}$, and correlation matrices, respectively:

$$e_1(\tilde{\boldsymbol{x}}, \boldsymbol{p}) = \sum_{i=1}^{d} \sum_{k=1}^{m} \left[\tilde{F}_i(\tilde{x}_{k,i}) - F_i(\tilde{x}_{k,i})\right]^2 \tag{5.10}$$

$$e_2(\tilde{\boldsymbol{x}}, \boldsymbol{p}) = \sum_{i=1}^{d} \sum_{r=1}^{\tilde{r}} [\tilde{\mu}_i(r) - \mu_i(r)]^2 \tag{5.11}$$

$$e_3(\tilde{\boldsymbol{x}}, \boldsymbol{p}) = \sum_{i,j=1\ldots d} \left[\tilde{\boldsymbol{r}}_{i,j} - \boldsymbol{r}_{i,j}\right]^2 \tag{5.12}$$

The coefficients $\alpha_u \geq 0$, $u = 1, 2, 3$ are weighting factors whose purpose is to make sure that each of the measures has the same order of magnitude, or to emphasize some of them if necessary.

The function *f* is then optimized to obtain the optimal SROM representation for *X*:

$$\tilde{X}_{SROM} = \tilde{X} = \left\{(\tilde{x}_k^{opt}, p_k^{opt})\right\}, \qquad 1 \leq k \leq m \tag{5.13}$$

5.2.Optimization procedures

In general, the optimal SROM can be constructed in three ways. Namely, the optimization can be done in a way that firstly samples are chosen in a somehow heuristic way and then the function *f* is optimized only over *p*:

$$\tilde{X} := \arg\min_{\boldsymbol{p}} f \tag{5.14}$$

This has been proposed in [12] and [46] (Section A.3) and used in [47]. The proposed algorithms are pattern classification, integer optimization and dependent thinning. Further details on each of the algorithms can be found in [12] and in references therein.

The second approach to optimization is completely heuristic, which is also the simplest one. It relies on the pattern classification algorithm that uses Voronoi tessellations to extract the samples as well as to calculate the probabilities without tackling the optimization problem in eq. (5.9). This approach is proposed in [46] (Section A.3).

Finally, the most optimal, but also the most complex way is to optimize the function *f* from eq. (5.9.) jointly over both $\{\widetilde{\boldsymbol{x}}\}$ and $\boldsymbol{p}$.

$$\tilde{X} := \arg\min_{\{\widetilde{\boldsymbol{x}}\}, \boldsymbol{p}} f \tag{5.15}$$

This approach has been reported in [48] and later used in [49] and [50].

5.3.Uncertainty propagation by SROM

This section outlines the two main ways of SROM uncertainty propagation to the output: "pure" SROM and Extended SROM (ESROM) [46] (Section A. 3 and A. 4). The first approach is based on piecewise constant approximation of the output of interest, while the second approach is based on piecewise linear approximation of the output. In addition, the output of interest can be approximated also by a piecewise quadratic approximation [51].

In the following text the output value is noted with *Y*, the corresponding SROM output construction with $\tilde{Y}$ and deterministic solver with *M*.

5.3.1. "Pure" SROM mapping

The main feature of this method is its simplicity. The input value is represented with SROM value-probability pairs $\tilde{X} = \{(\tilde{x}_k, p_k)\}$. Basically, deterministic solver is fed with the sample-probability pairs of the SROM input $\tilde{X}$ and the outcome is the sample-probability pair of the output value $\tilde{Y} = \{(\tilde{y}_k, p_k)\}$. The probabilities of the input are the same as for the output, since $\tilde{y}_k$ happens only if the $\tilde{x}_k$ is the current input. The mapping *X = M(Y)* can be formulated as the piecewise constant output function as follows:

$$\tilde{Y} = \sum_{k=1}^{m} \tilde{y}_k \, \mathbf{1}(X \in C_k) \tag{5.16}$$

where C_k is a measurable partition of the *X* domain such that $p_k = P\left(X^{-1}(C_k)\right), k = 1 \ldots m$.

Finally, the statistics of the output *Y* are approximated by using the SROM $\tilde{Y}$ and equations (5.6.)-(5.8.), which is step 3 on Fig.5.1. The scheme for the UP via SROM is depicted in the Fig. 5.1.

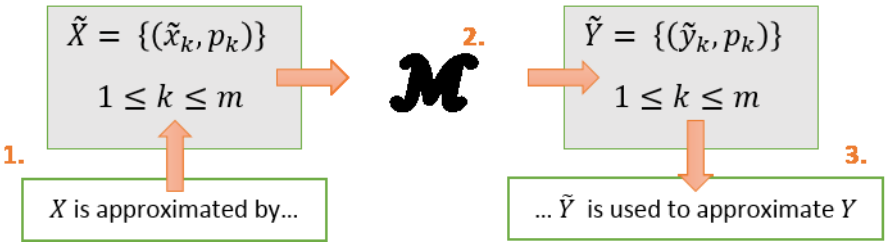

Figure 5.1. The "pure" SROM uncertainty propagation

5.3.2. Extended SROM mapping (ESROM)

Under assumption that mapping is sufficiently smooth the Extended SROM (ESROM) uses piecewise linear functions to approximate the $X = M(Y)$. This approach relies on the pattern classification and Voronoi tessellations for constructing the $\tilde{X} = \{(\tilde{x}_k, p_k)\}$. Once the input SROM has been constructed, m deterministic solutions $\tilde{y}_k$ are calculated as presented in Fig. 5.1. In addition, gradients of the output value with the respect to the coordinates of the input X have to be calculated:

$$\nabla\tilde{y}_k(\cdot) = \left[\frac{\partial\tilde{y}_k(\cdot)}{\partial x_1}, \dots, \frac{\partial\tilde{y}_k(\cdot)}{\partial x_d}\right] \quad 1 \le k \le m, \tag{5.17}$$

where d is the dimension, i.e. number of coordinates of the input variable.

Deterministic solutions $\{\tilde{y}_k\}$ and $\{\nabla\tilde{y}_k\}$ are then used for construction of local, linear piecewise approximation:

$$Y_L(\cdot) = \sum_{k=1}^{m}[\tilde{y}_k(\cdot) + \nabla\tilde{y}_k(\cdot) \cdot (X - \tilde{x}_k)]\,\mathbf{1}(X \in C_k) \tag{5.18}$$

The equation (5.18) gives the representation of $Y_L(\cdot)$ in each Voronoi cell C_k by a hyperplane tangent to $X \to Y$ at $(\tilde{x}_k, \tilde{y}_k), k = 1 \dots . m$ [9]. The ESROM scheme is depicted in Fig.5.2.

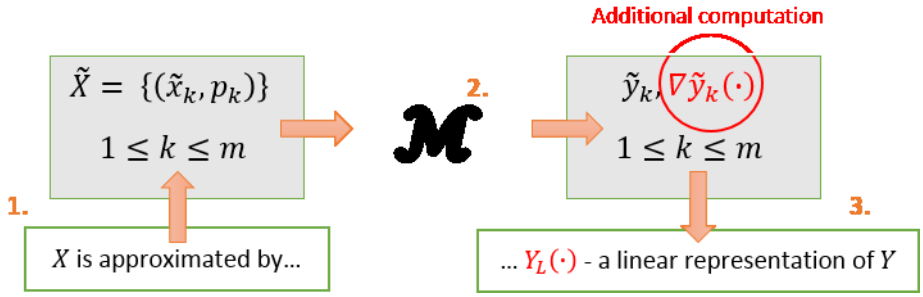

Figure 5.2. The extended SROM (ESROM) uncertainty propagation

5.4.Numerical example

For the purpose of illustration the SROM construction for the following random variables is given as an example: Gaussian random variable $X \sim N(0, 1)$ and beta random variable $X \sim B(5, 1)$. In each example the reconstructions of cdf and pdf are given and also the absolute error w.r.t. exact solutions for the first six stochastic moments. The SROM pdf is reconstructed by

using the values of SROM probabilities but scaled in order to compare it with the exact pdf on the same graph as it is the case for the exact solution. The algorithm described as the approach #2 is used for demonstration. The obtained results are suboptimal but it is evident that further work on optimization problem may result in even more accurate performance.

The results for the cdf and pdf in Figs. 5.3. and 5.5. are satisfactory thus proving that both cdf and pdf can be reconstructed by using relatively small number of SROM samples even when a suboptimal and simple approach #2 is used. On the other side, even though the absolute error of moments is good in most of examples (Figs. 5.4. and 5.6.), one may conclude that the behaviour of the error is not consistent with the rising number of samples. The expected trend for absolute error of moments is supposed to decrease both with the increasing number of samples and with increasing the moment order. The explanation can be found in the fact that the used algorithm does not solve the minimization function directly and there is no way to affect the moments' values.

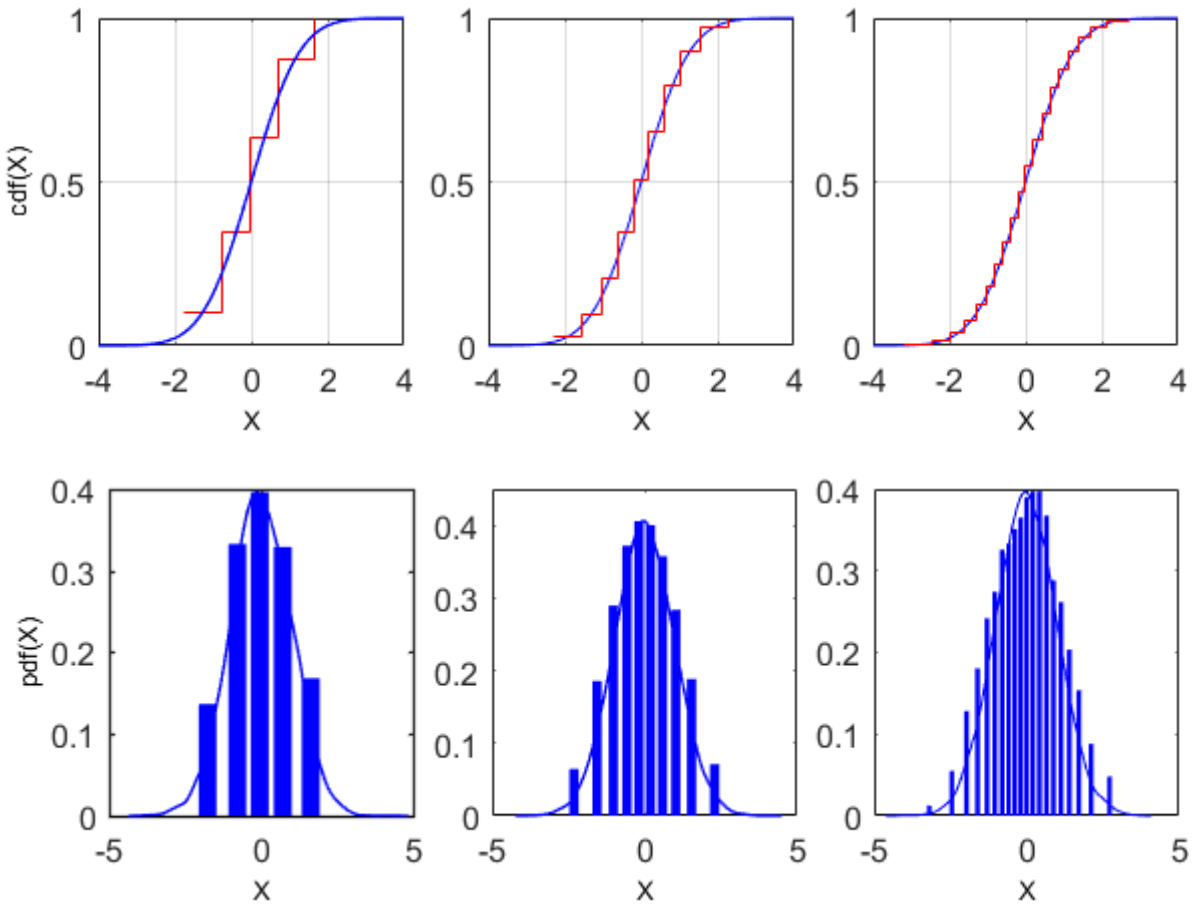

Fig. 5.3. The exact (blue) vs. SROM approximation (red) with 5, 10 & 20 samples (left to right) of cdf (top) and pdf (bottom) for the variable $X \sim N(0,1)$

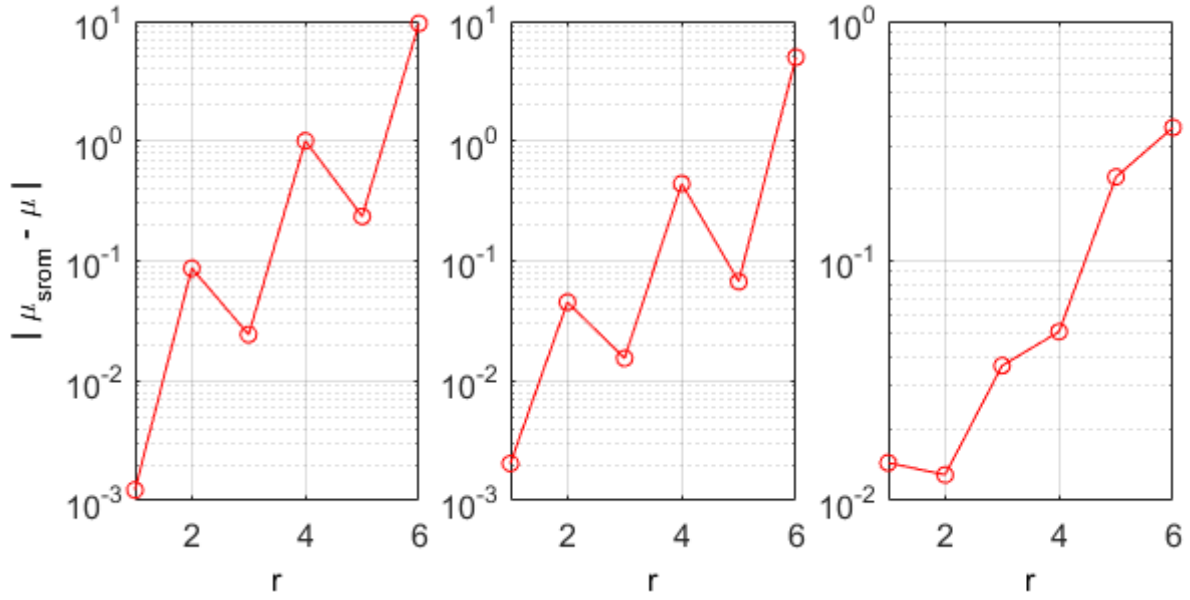

Fig. 5.4. The absolute error between the exact (blue) and SROM approximations (red) of first six stochastic moments for variable $X \sim N(0,1)$; SROM size is m=5,10 & 20, r=1,…6

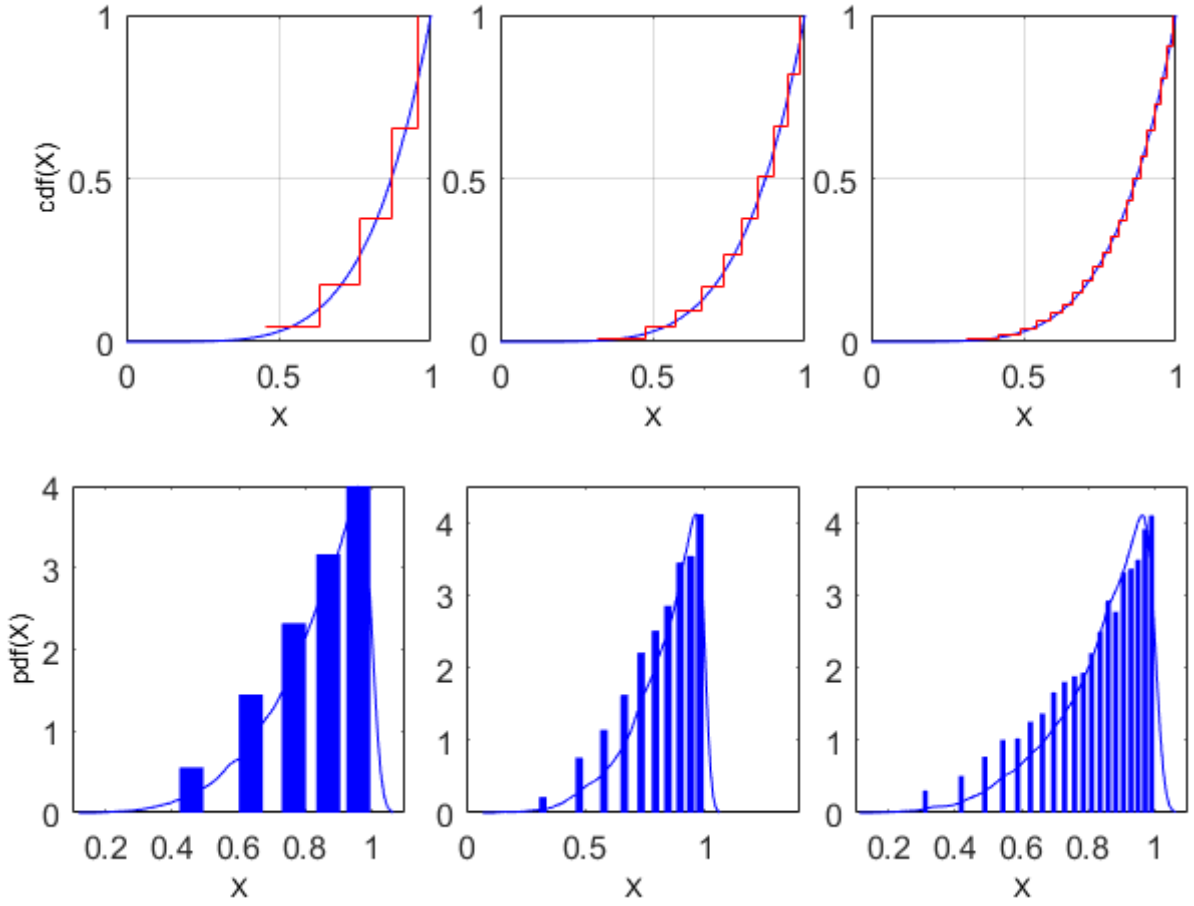

Fig. 5.5. The exact (blue) vs. SROM approximation (red) with 5, 10 & 20 samples (left to right) of cdf (top) and pdf (bottom) for the variable $X \sim B(5,1)$

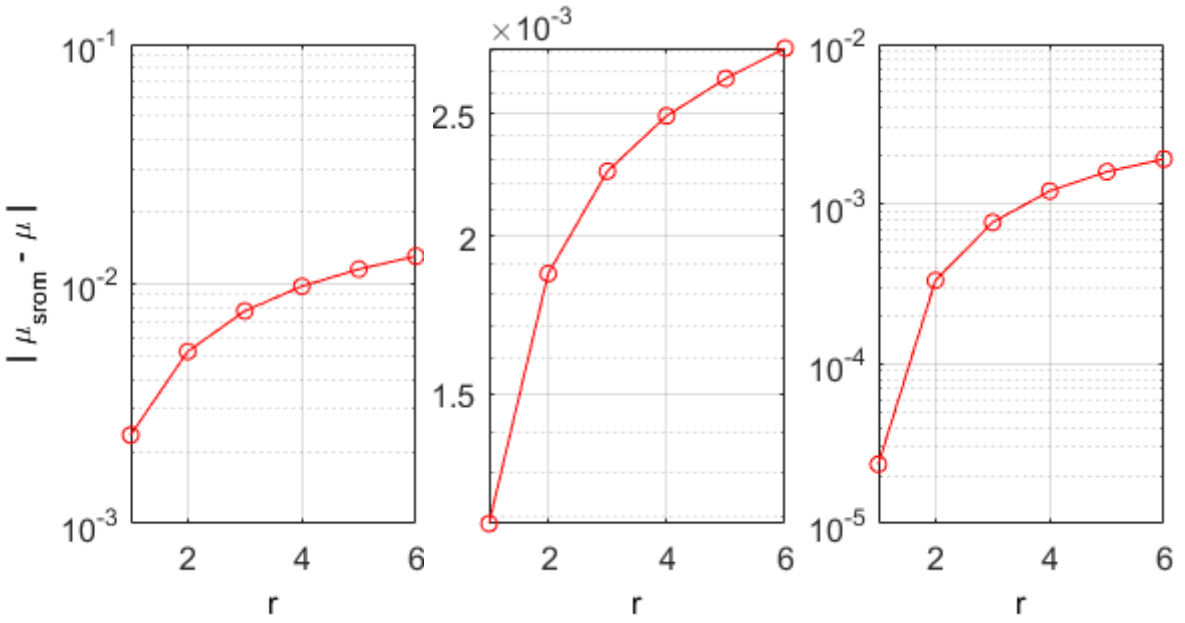

Fig. 5.6. The absolute error between the exact (blue) and SROM approximations (red) of first six stochastic moments for variable $X \sim B(5,1)$*; SROM size is m=5,10 & 20, r=1,…6*

6. State of the art

Some areas in computational electromagnetics (CEM) suffer from uncertainties of the input parameters resulting in the uncertainties in the assessment of the related response. The uncertainties are often related to the dielectric material characteristics [52], geometrical sizes [53] and boundary conditions [54]. The control of various uncertainties related to the models is important as it impacts optimization design and performance of electromagnetic structures and products. These problems have been faced, to a certain extent, by an efficient combination of well-established deterministic electromagnetic models with certain stochastic methods. This chapter gives an overview of some works related to the uncertainty analysis reported in the areas of CEM, mainly electromagnetic compatibility (EMC) and bioelectromagnetism (BIOEM).

6.1.Stochastic Analysis in Computational Electromagnetics

The stochastic analysis via the gPC and SC methods cover a wide range of EMC applications: the signal integrity, microwave applications, design of integrated circuits (IC), microelectromechanical systems (MEMSs) and photonic circuits, antenna modelling, scattering problems etc. Depending on the underlying problem, different variants of UQ techniques have been used with great progress regarding their optimization in recent years.

Various SC based techniques have been reported as promising UQ techniques in EMC area. The full-tensor SC has been used by Shen et al. for the stochastic analysis of variations of electromagnetic properties of composite mixtures [52], while Bonnet and his co-workers used it for numerical simulation of a reverberation chamber in [55]. Li and Jiang used the adaptive hierarchical sparse grid SC for the UQ of EM-circuit systems [56] combining the Lagrange and piecewise basis functions in order to build a more flexible UQ algorithm which can handle different stochastic systems. They verified the robustness of proposed approach on microwave circuits with microstrip interconnects, RLC resonant circuits and nonlinear power amplifiers. Also, they considered a far-field scattering of a dielectric sphere. A sparse grid SC was used by Agarwal and Aluru in [28] for stochastic analysis of electrostatic MEMS while Bai et al. proposed a dimension-reduced sparse grid SC method for EMC software [57]. M. Liu and S. Liu adopted the adaptive sparse grid method for the estimation of radar cross section (RCS) of object with uncertain shape [58].

The UQ of RCS, affected by the uncertainty in shape of the objects and by the direction of the incident field, was also considered by Chauviere and his co-workers in [29]. However, they used the SC method combined with Stroud cubature rule. The same approach was used by Bagci et al. in [59] for propagation of uncertainties in electromagnetic excitations, system geometries and configurations to the output coupled voltages at the feed pins of cable-interconnected and shielded computer cards as well as the terminals of cables situated inside the bay of an airplane cockpit. Prasad and Roy introduced a SPICE-compatible stochastic collocation approach based on Stroud cubature for the variability analysis of complex and irregular-shaped power distribution networks (PDNs) [60]. Zhang and his co-workers proposed a big-data tensor recovery technique defined as a tensor recovery problem with sparse and low-rank constraints solved with an alternating minimization approach [61]. They successfully applied it to simulation of some IC and MEMs with up to 50 random input parameter reducing the huge number of simulation samples in standard SC to a very small one (e.g., from 1.5 × 1027 to 500).

The examples of the gPC method applied to different areas in the EMC are numerous. Manfredi applied the gPC theory to the stochastic analysis of high-speed interconnect models with uncertain input parameters in his doctoral thesis [62]. An overview of the stochastic transmission line analysis via gPCE method may be found in [63]. A large number of uncertain input parameters was taken into account via the sparse polynomial chaos metamodel in the stochastic analysis of electronic bus by Larbi et al. [64]. In their recent work Prasad and Roy proposed a dimension reduction for efficient uncertainty analysis of microwave and RF networks in the polynomial chaos framework achieving better results w.r.t. classical sparse grids approach [65]. In [66] they addressed the issue of detecting and quantifying the mixed epistemic-aleatory uncertainties in the multiconductor transmission line networks by building a hybrid Chebyshev-polynomial chaos (CPC) metamodel. Petrocchi et al. carried out the analysis of the propagation of measurement uncertainty in microwave transistor nonlinear models [67]. They used gPC method and compared the results with the NIST Microwave Uncertainty Framework showing a significant reduction of the computational effort in case of gPC use. An adaptive least angle regression method for UQ in FDTD computation is proposed by Hu et al. in [68]. The variability of crosstalk due to changes in differential and ground via configurations is studied in [69] by using two UQ methods: gPC and response-surface method. The challenge of dealing with data coming from a real-time measurments was tackled by Alkhateeb and Ida in [70]. They proposed a multi-element arbitrary polynomial chaos (ME-aPC) scheme for uncertainty quantification in sensors. Acikgoz and Mittra applied gPC

technique to a conducting array of split-ring resonator to study the effect of the uncertainties of its design parameters on its reflectance at terahertz frequencies [71].

Beside the gPC and SC methods, the SROM method has been introduced to the EMC by Fei and his co-authors. They used SROM for the analysis of an induced current in transmission line illuminated by a random plane-wave field [72] and for uncertainty quantification of crosstalk [73]. In their work they based SROM approach on a heuristic algorithm described as approach no.2 in section 5 and compared it with MC and SC methods. The results obtained by SROM were comparable to those of MC and SC approaches but with less input samples thus indicating a good potential of SROM based methods in this area.

6.2.Stochastic Analysis in Bioelectromagnetism

The use of electromagnetic (EM) fields in everyday life increases the constant public concern regarding their potential harmful effects on the human health. The nature of interaction between the EM fields and the human body is different at high and low frequency ranges (HF and LF). In the HF range body dimensions are comparable to the external field wavelength and the resonance effects become significant thus making the thermal effects dominant. In the LF range, however, the non-thermal effects could possibly have severe influence on the membrane cells. As an example, international standards and guidelines for HF exposure list the human brain as one of the most sensitive organs to the temperature variations. Contrary to the possible adverse health effects, the EM fields are often used in therapeutic purposes. One such example is the transcranial magnetic stimulation (TMS), a noninvasive and painless technique used for stimulation or inhibition of certain brain regions.

Regardless the nature of EM field interaction with the human body, the understanding of it depends on the numerical and computational models. However, the input parameters of models used in bioelectromagnetism and EM dosimetry are by their very nature uncertain. The values of body tissue parameters such as permittivity and the electrical conductivity vary significantly, depending on the age and gender, but also between healthy and ill individuals. Most of the parameter values presented in overviews like [74] are obtained under different measurement on ex vivo animal and human tissues, and exhibit large variations from their averages [75]. When used in computational models, these average values lead to rough approximation of the real situation [76] [77].

Beside the body tissue parameters, the sources of radiation also exhibit random nature. The position and the orientation of antennas have different impact on the resulting induced fields [78]. In the process of quantification of people's exposure to complex environment, it is necessary to take into account the specific probability distribution of the angle of incidence and magnitude of electromagnetic waves [79]. Furthermore, a well-functioning wireless network demands the prediction of its coverage, capacity and throughput. Therefore in the numerical simulation a concept of stochastic city model is used which takes into account the random nature of built surface, height of building or length of streets [80].

The models used in bioelectromagnetism and numerical dosimetry are computationally very demanding as they describe a very complex physical phenomena and environments. Despite the progress in high-performance calculation (HPC), uncertainty quantification based on traditional Monte Carlo method presents an enormous burden which is often unaffordable. Therefore the UQ methods such as gPC and SC have become of interest to many researchers in this area. The combination of the advanced electromagnetic solvers and the statistic tools have led to a novel approach called the stochastic dosimetry [81] enabling the faster computation of the stochastic moments, probability distribution and confidence intervals of specific absorption rate (SAR). In [82] Wiart et al. used a gPC method to characterize the statistical distribution of the SAR in children organs exposed to mobile phones in pockets with random position. Chiaramello and her co-workers utilized the gPC methodology to quantify the fetal exposure to a fourth-generation Long Term Evolution (4G LTE) tablet in realistic scenarios, assessing the influence of the position of the tablet, the gestational age of the fetus, and the frequency of the emitting antenna [78]. They also investigated the exposure of a female eight-year old child to a WLAN access point located in an unknown position in a realistic indoor environment in [83]. Cheng and Monebhurrun conducted the UQ of SAR using a computer-aided design mobile phone model by three nonintrusive UQ methods: unscented transformation, stochastic collocation, and nonintrusive polynomial chaos [84].

Given that the temperature evaluation is a direct consequence of tissue heating, one important aspect of the HF numerical dosimetry is its evaluation. In order to do so, a bioheat transfer equation needs to be solved which includes certain thermal parameters of body tissues as the input variables. The effect of tissue parameters on skin heating due to millimeter EM waves was investigated by Zilberti et al. in [85].

The uncertainty of tissue electric parameters for UQ of the induced fields and current densities in human body due to ELF EMF has been taken into account by Gaignaire et al. in

[86]. By using the Hermite polynomial chaos they showed the probability of the induced fields to be over the thresholds defined by the international guidelines for limiting exposure to electromagnetic fields published by ICNIRP. Lallechere and his co-workers utilized a stochastic collocation method to propagate uncertainty of tissue electric parameters in stochastic modelling of biological cell subjected to pulsed EMF exposure [87].

The UQ of the fields induced in the human brain due to the exposure to coils used in TMS has been investigated by Weise et al. in [88] and Codecasa et al. in [89]. They modelled the conductivity of cerebrospinal fluid, gray matter and white matter as uniformly distributed random variables and propagated the uncertainty to the induced electric field via the nonintrusive gPC method. Their results showed the importance of exact knowledge of the electrical conductivities in TMS in order to provide reliable numerical predictions of the induced electric field. Moreover, in [90] they accounted for the correlation between the tissue conductivities. In addition to tissue conductivity, Gomez and his co-workers considered the variability of coil position and orientation and bran morphology [91] by using the high-dimensional model representations via a multielement probabilistic collocation (ME-PC) method. They reported the following implications of the UQ results for the use of TMS during depression therapy: 1) uncertainty in the coil position and orientation may reduce the response rates of patients; 2) practitioners should favor targets on the crest of a gyrus to obtain maximal stimulation; and 3) an increasing scalp-to-cortex distance reduces the magnitude of E-fields on the surface and inside the cortex. The UQ of induced electric field in human brain due to uncertain TMS coil position and orientation via the multi-variate gPC expansions was considered by Li and Wu [92].

Beside the simulation of TMS, the UQ has been reported in simulation of some other biomedical applications of EMF, as well. To mention some, Aboulaich et al. studied the influence of errors and uncertainties of the input data, like the conductivity, on the electrocardiography imaging (ECGI) solution [93]. Schmidt and co-workers presented a computational models of an electrostimulative total hip revision system to enhance bone regeneration in [94]. They utilized gPC method to investigate the influence of uncertainty in the conductivity of bone tissue on the electric field strength and the beneficial stimulation volume for an optimized electrode geometry and arrangement.

Furthermore, the uncertainty quantification of tissue dialectical properties has been reported in [95] by Arduino et al. They employed Monte Carlo method for uncertainty propagation in magnetic resonance-based electric properties tomography. Merla et al. proposed a stochastic

EM solution based on MC method for uncertainty estimation in microdosimetric study on erythrocytes [96].

In conclusion, all of the mentioned works indicate the importance of the exact knowledge of the electrical parameters of body tissues and sources of EM radiation. By taking into account their random nature and propagating it to the output we can increase our knowledge about the underlying physical processes and quantify their impact on reliability of numerical predictions of the induced electric field and related quantities.

7. Case study: Stochastic Sensitivity Analysis of 1D Bioheat Transfer Equation

The knowledge about the temperature distribution is an important issue in planning and modelling of biomedical applications of electromagnetic (EM) fields, e.g. EM HyperThermia (EM HT) procedures used in the treatment of certain cancer types [97]. In order to model the interactions of EM fields with the body tissue in the EM HT process it is important to use values of the dielectric and thermal tissue properties as accurate as possible. Hence, it is important to incorporate the uncertainties in the tissue thermal parameters and quantify the uncertainty in the output temperature. Such an information can be useful when estimating the technical risk of medical devices and when optimizing their design regarding the efficacy and safety.

A stochastic model of the bioheat transfer equation to assess the temperature distribution in the biological tissue is presented in this subsection. The stochastic collocation method is implemented to estimate the stochastic mean and variance, as well as, to carry out the sensitivity analysis of model. The presented stochastic model and the related results have been published in [98].

7.1.Stochastic bio-heat equation

The theoretical background for the modelling of heat transfer in the biological tissues relies upon the Pennes' bioheat equation. In this case study the 1-dimensional bioheat equation governing the temperature distribution in the human skin is considered:

$$\frac{d^2T(x)}{dx^2} - w_b \cdot T(x) + w_b \cdot T_a + Q_m + Q_{ext} = 0 \tag{7.1}$$

where λ stands for the skin thermal conductivity, w_b is the volumetric perfusion blood rate, T_a is the arterial temperature and Q_m is the heat source due to metabolic processes. The term, Q_{ext}, represents the external heat source. In case of EM HT treatment this term represents the heat due to the influence of the EM field. For the present case study this term shall be equal to zero.

The corresponding boundary conditions at the interface between the model surface and the air *(x=L)* are given as:

$$T(x = 0) = T_c \tag{7.2}$$

$$-\lambda \cdot \left.\frac{dT(x)}{dx}\right|_{x=L} = h_{eff} \cdot [T - T_{amb}]$$

where h_{eff}, T_c and T_{amb} are: the convection coefficient, the body core temperature, and the air temperature, respectively.

The deterministic bio-heat equation (7.1.) is solved by means of finite element method (FEM). The output of interest is the temperature distribution for a single setup of input parameters.

However, in order to take into account the uncertainty present in the input parameters that describe certain tissue type, the equation should be treated as stochastic. The thermal parameters: λ, w_b, T_a, O_m, h_{eff} and T_f are modelled as random variables (RV) with uniform distribution in the range of ± 20% from their nominal values which are given in the Table 7.1. The random input vector is thus given as: $\boldsymbol{X} = [x_1, x_2, x_3, x_4, x_5, x_6] = [\lambda, w_b, T_a, Q_m, h_{eff}, T_{amb}]$. The skin depth is considered to be $L = 3\ cm$.

Table 7.1. The nominal values for the thermal parameters

Thermal parameter			**Nominal value**
thermal conductivity	λ	[W/m°C]	0.5
volumetric perfusion blood rate	w_b	[kg/(sm^3)]	2100
arterial temperature	T_a	[°C]	37
heat source due to metabolic processes	Q_m	[W/m^3]	33800
convection coefficient	h_{eff}	[W/(m^2 °C)]	10
ambient temperature	T_{amb}	[°C]	25

7.2.The results of stochastic computations

The SC method is used as a wrapper around the deterministic code for the assessment of the stochastic response. Lagrange polynomials are chosen as basis functions, while collocation points in each dimension are chosen according to Gauss-Legendre or Clenshaw-Curtis quadrature rules for tensor or sparse grid products, respectively. The chosen sparseness parameter for sparse grid construction is $q = 3$.

The full-tensor SCM resulted in 729 deterministic simulations and sparse-grid SCM in 389 simulations. The MCM method is used as a validation in the following way: 100 sets of MC simulations are computed, each with 1.000 samples. The reference mean and variance are taken from one MC simulation set with 1.000.000 samples.

7.2.1. Stochastic moments of the output temperature

The results for the mean and variance of temperature distribution are shown in Figs. 7.1. and 7.2. The quick convergence of the SCM w.r.t. MC simulations is obvious, particularly in the computation of stochastic variance.

The crude estimation of the confidence intervals (CI) given as the mean value ± 1 standard deviation is shown in Fig.7.3. The maximal deviation is 6.43% from the mean value.

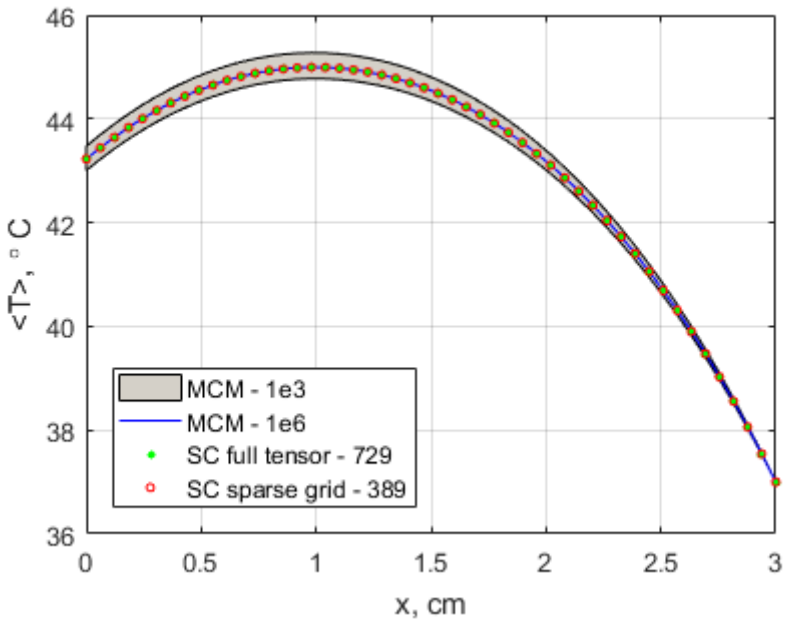

Fig. 7.1. The mean value of the temperature distribution in the skin tissue obtained by MCM, full-tensor SCM and a sparse-grid SCM

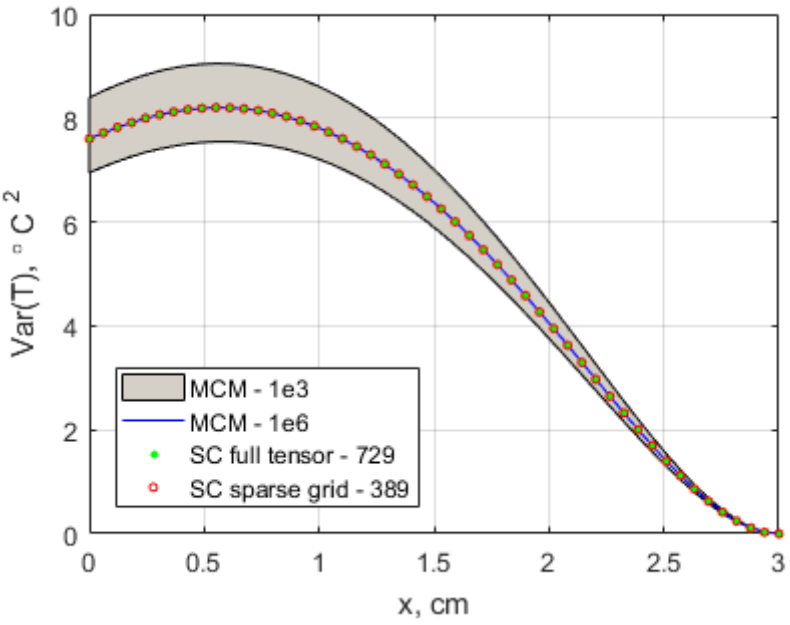

Fig. 7.2. The variance of the temperature distribution in the skin tissue obtained by MCM, full-tensor SCM and a sparse-grid SCM

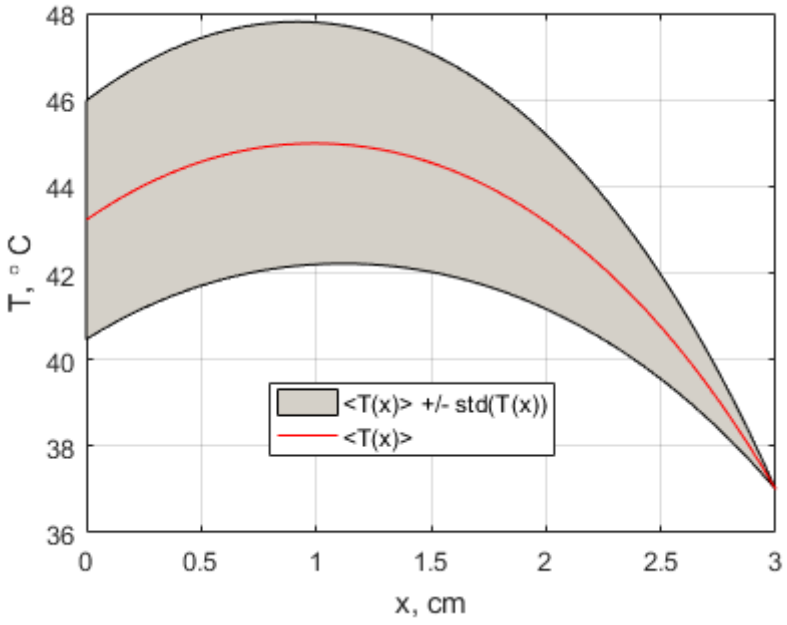

Fig. 7.3. The confidence intervals (CI) given as the mean temperature ± 1 standard deviation of the temperature: <T> ± std(T). The results are obtained by using sparse grid SCM.

7.2.2. Sensitivity analysis of thermal parameters

The influence of the variation in the input variables on the output temperature distribution is computed both by using the OAT and ANOVA approaches described in the section 2. The results for the OAT based approach are depicted on the left side of the figure 7.4. For each of the six univariate cases the mean ± one standard deviation is given, thus illustrating the wideness of the confidence interval range for each case.

On the right side of the Fig. 7.4. the distribution of the first order sensitivity index values along the skin tissue is depicted for each input random variable. The sensitivity indices are obtained by means of ANOVA based approach combined with SC framework.

The accuracy of the ANOVA based approach within the SC framework was validated against the Sobol's sensitivity indices computed via MC based sampling for the first order and total effect sensitivity indices. The total number of MC samples is 1000 The results are depicted in the Figs. 7.5. and 7.6.

The results of sensitivity analysis demonstrate the overwhelming impact of arterial temperature over the whole domain followed by the influence of metabolic processes, both in a homogenous trend. Other parameters exhibit nonhomogeneous influence. The values of total and first order indices are almost the same for each parameter, thus proving that none of the mutual interactions has a significant impact on the temperature distribution.

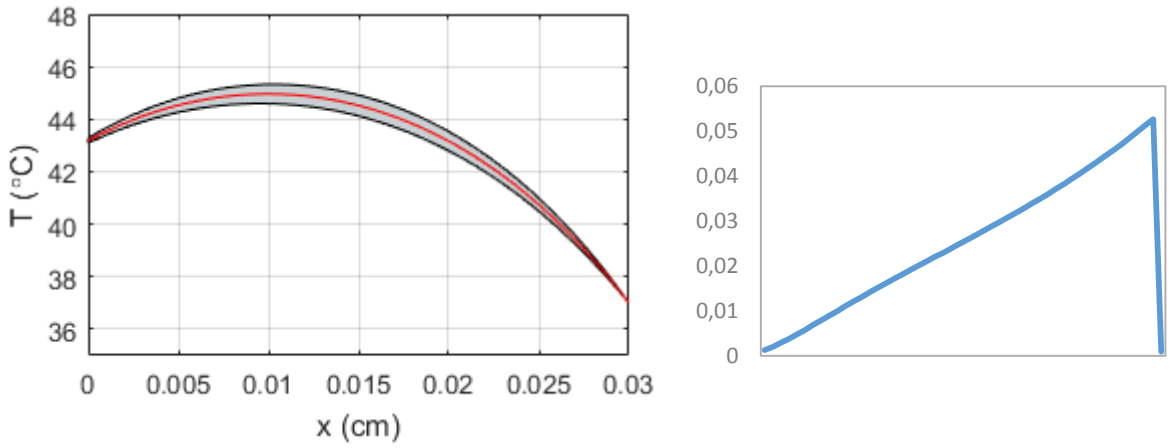

a) Skin thermal conductivity, λ

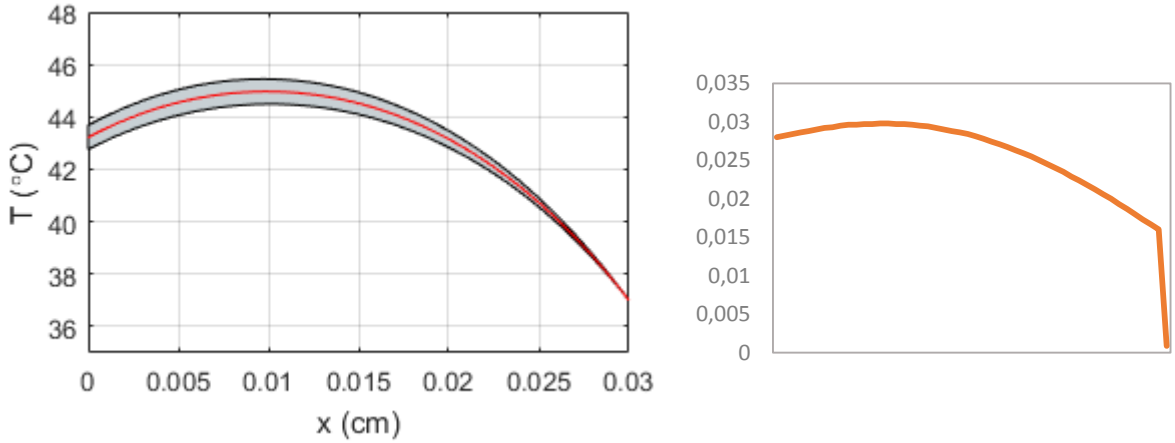

b) Volumetric perfusion blood rate, W_b

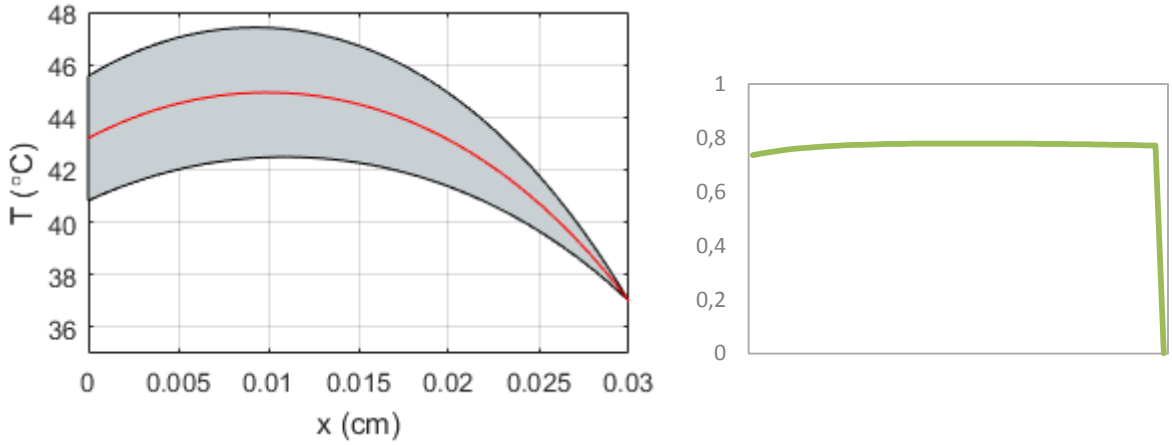

c) Arterial blood temperature, T_a

Fig. 7.4.(a-c) The confidence intervals defined as mean value ± one standard deviation for six univariate cases (left) and the distribution of the first order sensitivity index for each random input variable along the skin depth (right)

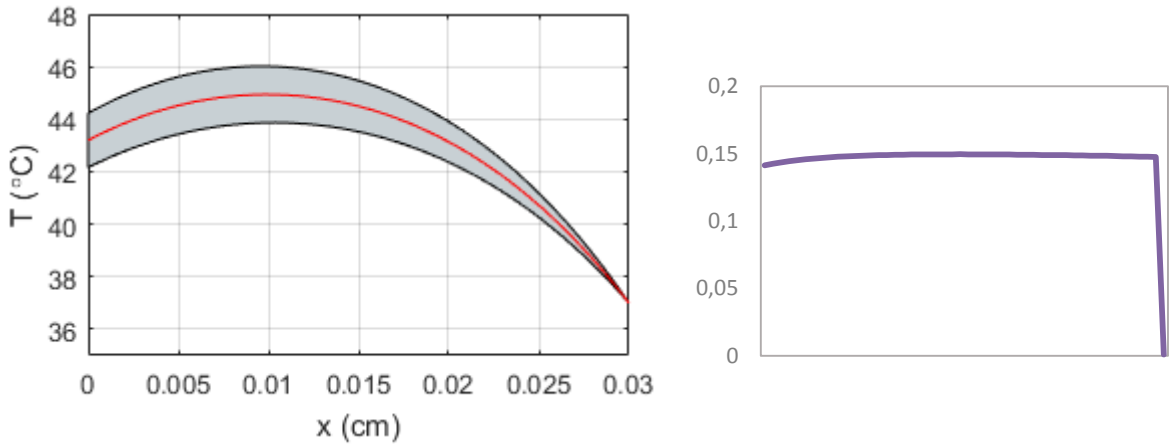

d) The heat source due to metabolic processes, Q_m

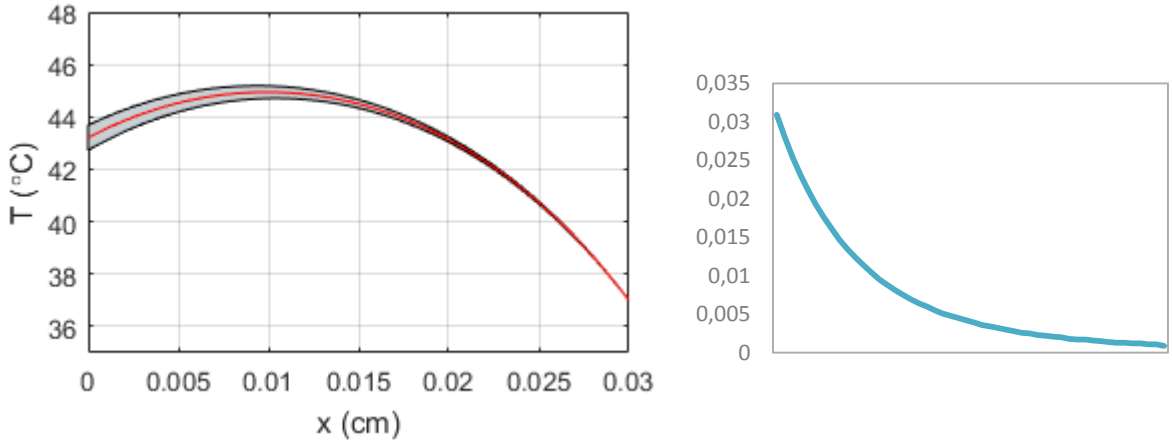

e) The convection coefficient, h_{eff}

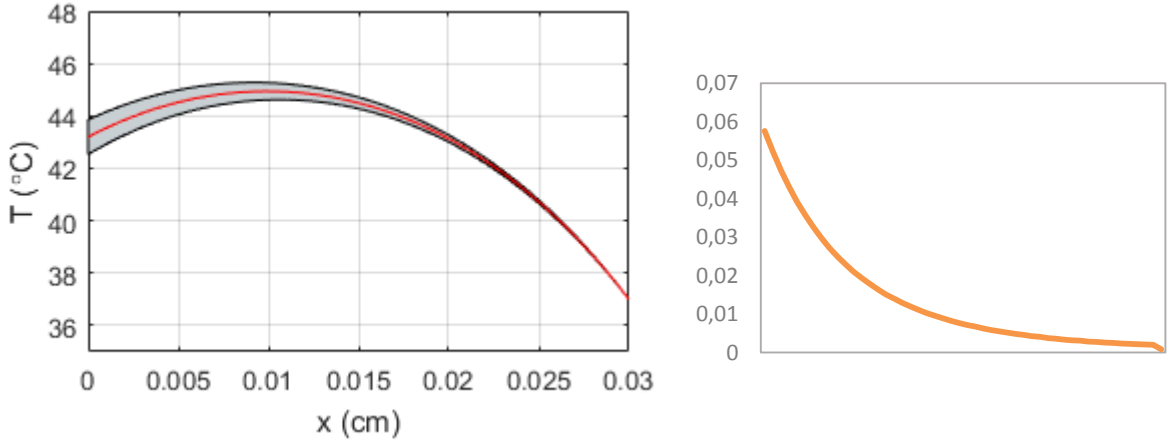

f) The ambient temperature, T_{amb}

Fig. 7.4.(d-f) The confidence intervals defined as mean value ± one standard deviation for six univariate cases (left) and the distribution of the first order sensitivity index for each random input variable along the skin depth (right)

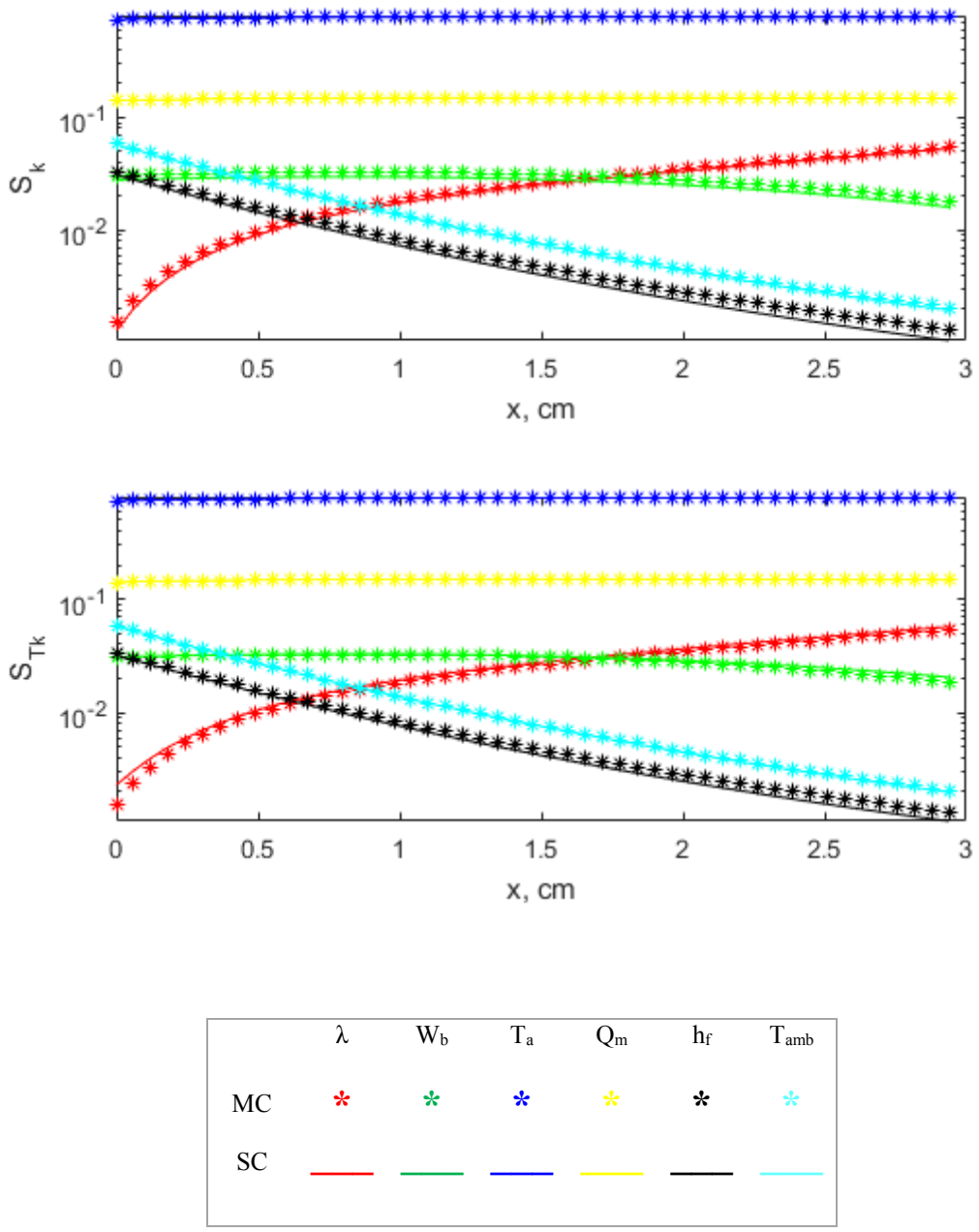

Fig. 7.5. The Sobol-like sensitivity indices at every point along the skin computed by MC and SC method: first order sensitivity index (top) and total effect sensitivity index (bottom)

8. Conclusion

A continuous interest in the topics pertaining to uncertainty in engineering has resulted in growing number of theoretical and experimental studies in this area. Thus, over the last few years uncertainty quantification has been introduced in several engineering disciplines due to the complexity of physical phenomena. Namely, significant discrepancies between calculated and measured results stem from uncertainties in the input data set arising from numerical instabilities, geometry, manufacturing defects, noise in measurements, unpredictable and uncontrollable environmental effects, etc.

This work reviews some applications of uncertainty quantification (UQ) methods in the area of computational electromagnetics and bioelectromagnetism. Besides the wide range of UQ applications, the development of three UQ methods and their respective variants has been described. Namely, the basic concepts of generalized polynomial chaos (gPC), stochastic collocation method (SCM) and stochastic reduced order model (SROM) method are given. Furthermore the "one-At-a-Time" (OAT) and the "Analysis Of Variance" (ANOVA) based approaches for sensitivity analysis are outlined.

A state of the art for the stochastic analysis in the computational electromagnetics and bioelectromagnetism demonstrates the importance of the exact knowledge of the electrical parameters of materials, geometry and sources of EM radiation. By taking into account their random nature and propagating it to the output we can increase our knowledge about the underlying physical processes and quantify their impact on reliability of numerical predictions of the related output quantities.

The example of UQ for the stochastic bioheat transfer equation, given in the last chapter, clearly demonstrates the efficiency of stochastic collocation method w.r.t. traditional Monte Carlo method.

Bibliography

[1] G. Iaccarino, *Uncertainty Quantification in Simulations of Reactive Flows,* Marseille, 2012.

[2] A. Papoulis, Probability, Random Variables and Stochastic Processes, New York: McGraw-Hill, Inc, 1991.

[3] R. G. Ghanem and P. D. Spanos, Stochastic Finite Elements: A Spectral Approach, New York: Springer-Verlag, 1991.

[4] B. Sudret and A. Der Kiureghian, "Stochastic Finite Element Methods and Reliabiltiy," Report Report No. UCB/SWMM-2000/08, Departmetn of Civil & Environmental Engineering, University of California, Berkley, 2000.

[5] B. Sudret, "Polynomial Chaos Expansions and Stochastic Finite Element Methods," Risk and Reliability in Geotechnical Engineering (Chap. 6), K.-K. Phoon & J. Ching (Eds.), pp. 265-300, CRC Press., Zurich, 2014.

[6] D. Xiu, "Fat Numerical Methods for Stochastic Computations: A Review," *Commun. Comput. Phys,* vol. 5, no. 2-4, pp. 242-272, Feb 2009.

[7] D. Xiu and G. E. Karniadakis, "The Wiener--Askey Polynomial Chaos for Stochastic Differential Equations," *SIAM Journal on Scientific Computing,* vol. 24, no. 2, pp. 614-644, October, 2002.

[8] L. Mathelin and M. Y. Hussaini, "A Stochastic Collocation Algorithm fo Uncertainty Analyis," NASA Center for AeroSpace Information, Hanover, 2003.

[9] M. S. Eldred and J. Bukardt, "Comparison of Non-Intrusive Polynomial Chaos and Stochastic Collocation Methods for Uncertainty Quantification," in *47th AIAA Aerospace Sciences Meeting including The New Horizons Forum and Aerospace Exposition*, Orlando, Florida, 2009.

[10] J. Bai, G. Zhang, D. Wang, A. P. Duffy and L. Wang, "Performance Comparison of the SGM and the SCM in EMC Simulation," *IEEE Transactions on Electromagnetic Compatibility,* vol. 58, no. 6, pp. 1739 - 1746, 2016.

[11] P. Manfredi, D. De Zutter and D. Vande Ginste, "On the relationship between the stochastic Galerkin method and the pseudo-spectral collocation method for linear differential algebraic equations," *Journal of Engineering Mathematics,* vol. 108, no. 1, pp. 73-90, 2018.

[12] M. Grigoriu, "Reduced order models for random functions. Application to stochastic probelms," *Applied Mathematical Modelling,* vol. 33, pp. 161-175, 2009.

[13] R. Jr., M. Grigoriu and J. M. Emery, "On the efficiacy of stochastic collocation, stochastc Galerkin, and stochastic reduced order models for solving stochastic problems," *Probabilistic Engineering Mechanics,* vol. 41, p. 2015, 60-72.

[14] R. Trinchero, M. Larbi, H. M. Torun, F. G. Canavero and M. Swaminathan, "Machine Learning and Uncertainty Quantification for Surrogate Models of Integrated Devices With a Large Number of Parameters," *IEEE Access (Volume: 7), 2018, doi: 10.1109/ACCESS.2018.2888903,* vol. 7, pp. 1-12, 2018.

[15] I. M. Sobol, A Primer for the Monte Carlo Method, Boca Raton, Florida, USA: CRC Press, Inc., 1994.

[16] M. H. Kalos and P. A. Whitlock, The Monte Carlo Methods, Hoboken, NJ: Wiley, 2008.

[17] A. Saltelli, M. Ratto, T. Andres, F. Campologno, F. Cariboni, D. Gatelli, M. Saisana and S. Tarantola, Global Sensitivity Analysis: The Primer, West Susex, England: John Wiley & Sons, Ltd, 2008.

[18] I. M. Sobol, "Sensitivity Estimates for Nonlinear Mathematical Models," *Matematicheskoe Modelirovanie. 2.,* p. 112–118, 1990.

[19] W. N., "The Homogeneous Chaos," *American Journal of Mathematics,* vol. 60, no. 4, pp. 897-936, 1938.

[20] R. H. Cameron and W. T. Martin, "Transformations of Wiener Integrals under Translations," *Annals of Mathematics,* vol. 45, no. 2, pp. 386-396, 1944.

[21] I. Babuška, R. Tempone and G. E. Zouraris, "Galerkin Finite Element Approximations of Stochastic Elliptic Partial Differential Equations," *SIAM Journal on Numerical Analysis,* vol. 42, no. 2, pp. 800-825, 2004.

[22] O. P. Le Maitre, O. Knio, H. Najm and R. Ghanem, "Uncertainty propagation using Wiener–Haar expansions," *Journal of Computational Physics,* vol. 197, no. 1, pp. 28-57, 2004.

[23] X. Wan and G. E. Karniadakis, "Multi-Element Generalized Polynomial Chaos for Arbitrary Probability Measures," *SIAM Journal on Scientific Computing,* vol. 28, no. 3, pp. 901-928, 2006.

[24] B. Sudret, "Global sensitivity analysis using polynomial chaos expansion," *Reliability Engineering & System Safety,* vol. 93, no. 7, pp. 964-979, 2008.

[25] D. Xiu, "Efficient collocation approach for parametric uncertainty analysis," *Communications in Computational Physics,* vol. 2, no. 2, pp. 293-309, 2007.

[26] D. Xiu and J. S. Hesthaven, "High-Order Collocation Methods for Differential Equations with Random Inputs," *SIAM Journal on Scientific Computing,* vol. 27, no. 3, pp. 1118-1139, 2005.

[27] M. Gunzburger, C. G. Webster and G. Zhang, "An adaptive wavelet stochastic collocation method for irregular solutions of stochastic partial differential equations," Oak Ridge National Laborator, Oak Ridge, Tennessee , 2012.

[28] N. Agarwal and N. R. Aluru, "Stochastic Analysis of Electrostatic MEMS Subjected to Parameter Variations," *Journal of Microelectromechanical Systems,* vol. 18, no. 6, pp. 1454-1468, 2009.

[29] C. Chauvire, J. S. Hesthaven and L. C. Wilcox, "Efficient Computation of RCS From Scatterers of Uncertain Shapes," *IEEE Transactions on Antennas and Propagation,* vol. 55, no. 5, pp. 1437-1448, 2007.

[30] G. T. Buzzard and D. Xiu, "Variance-Based Global Sensitivity Analysis via Sparse-Grid Interpolation and Cubature," *Communications in Computational Physics,* vol. 9, no. 3, pp. 542-567, 2011.

[31] G. Tang, G. Iaccarino and M. S. Eldred, "Global Sensitivity Analysis for Stochastic Collocation Expansion," in *Proceedings of the 51st AIAA/ASME/ASCE/AHS/ASC Structures, Structural Dynamics, and Materials Conference*, Orlando, Florida, 2010.

[32] M. Iglesias and A. M. Stuart, "Inverse Problems and Uncertainty Quantification," *SIAM NEWS ,* July/August 2014.

[33] X. Ma and N. Zabaras, "An efficient Bayesian inference approach to inverse problems based on an adaptive sparse grid collocation method," *Inverse Problems,* vol. 25, no. 2009, pp. 1-27, 2009.

[34] Y. M. Marzouk and D. Xiu, "A Stochastic Collocation Approach to Bayesian Inference in Inverse Problems," *Communications in Computational Physics,* vol. 6, no. 4, pp. 826-847, 2009.

[35] L. Yan and L. Guo, "Stochastic Colloation Algorithms using L1-minimization for Bayesian Solution of Inverse Problems," *SIAM Journal on Scientific Computing,* vol. 37, no. 3, p. 26, 2015.

[36] M. A. Tatang, W. Pan, R. G. Prinn and J. McRae, "An efficient method for parametric uncertainty analysis of numerical geophysical models," *Journal of Geophysical Research,* vol. 102, no. D18, pp. 21925-21932, 1997.

[37] I. Babuška, F. Nobile and R. Tempone, "A Stochastic Collocation Method for Elliptic Partial Differential Equations with Random Input Data," *SIAM Journal on Numerical Analysis,* vol. 45, no. 3, pp. 1005-1034, 2007.

[38] S. A. Smolyak, "Quadrature and interpolation formulas for tensor products of certain classes of functions," *Doklady Akademii Nauk SSSR,* vol. 148, no. 5, pp. 1042-10445, 1963.

[39] V. Barthelmann, E. Novak and K. Ritter, "High Dimensional Polynomial Interpolation on Sparse Grids," *Advances in Computational Mathematics,* vol. 12, no. 4, pp. 273-288, 2000.

[40] E. Novak and K. Ritter, "Simple Cubature Formulas with High Polynomial Exactness," *Constructive Approximation,* vol. 15, no. 4, pp. 499-522, 1999.

[41] J. Garcke and M. Griebel, Sparse Grids and Applications, Bonn: Springer Science & Business Media, 2012.

[42] C. Zenger, *Sparse grids,* Kiel: W. Hackbusch, editor, Parallel Algorithms for Partial Differential Equations, Proceedings of the Sixth GAMM-Seminar, 1991.

[43] R. Cools, "An encyclopaedia of cubature formulas," *Journal of Complexity,* vol. 19, no. 3, pp. 445-453, 2003.

[44] A. H. Stroud, Approximate Calculation of Multiple Integrals, Englewood Cliffs, NJ: Prentice–Hall, 1971.

[45] M. Grigoriu, "Solution of linear dynamic systems with uncertain properties by stochastic reduced order models," *Probabilistic Engineering Mechanics,* vol. 34, pp. 168-176, 2013.

[46] M. Grigoriu, Stochastic Systems: Uncertainty Quantification and Propagation, Springer, 2012.

[47] M. Grigoriu, "A method for solving stochastic equations by reduced order models and local approximations," *Journal of Computational Physics,* vol. 231, no. 19, pp. 6495-6513, 2012.

[48] . J. E. Warner, M. Grigoriu and W. Aquino, "Stochastic reduced order models for random vectors: Application to random eigenvalue problems," *Probabilistic Engineering Mechanics,* vol. 31, pp. 1-11, 2013.

[49] S. Sarkar, J. E. Warner, W. Aquino and M. Grigoriu, "Stochastic reduced order models for uncertainty quantification of intergranular corrosion rates," *Corrosion Science,* vol. 80, pp. 257-268,, 2014.

[50] J. E. Warner,, W. Aquino and M. Grigoriu, "Stochastic reduced order models for inverse poblems under uncertainty," *Computer Methods in Applied Mechanics and Engineering,* vol. 285, pp. 488-514, 2015.

[51] R. V. Field Jr., M. Grigoriu and J. M. Emery, "On the efficiacy of stochastic collocation, stochastc Galerkin, and stochastic reduced order models for solving stochastic problems," *Probabilistic Engineering Mechanics,* vol. 41, pp. 60-72, 2015.

[52] J. Shen, H. Yang and J. Chen, "Analysis of Electrical Property Variations for Composite Medium Using a Stochastic Collocation Method," *IEEE Transactions on Electromagnetic Compatibility ,* vol. 54, no. 2, pp. 272-279, 2012.

[53] D. H. Mac, S. Clenet, J. C. Mipo and I. Tsukerman, "A Priori Error Indicator in the Transformation Method for Problems With Geometric Uncertainties," *IEEE Transactions on Magnetics,* vol. 49, no. 5, pp. 1597-1600, 2013.

[54] L. Tenuti, N. Anselmi, P. Rocca, M. Salucci and A. Massa, "Minkowski Sum Method for Planar Arrays Sensitivity Analysis With Uncertain-But-Bounded Excitation Tolerances," *IEEE Transactions on Antennas and Propagation,* vol. 65, no. 1, pp. 167-177, 2017.

[55] P. Bonnet, S. Lallechere, C. Chauviere and F. Diouf, "Numerical simulation of a Reverberation Chamber with a stochastic collocation method," *Comptes Rendus Physique,* vol. 10, no. 1, pp. 54-54, 2009.

[56] P. Li and L. J. Jiang, "Uncertainty Quantification for Electromagnetic Systems Using ASGC and DGTD Method," *IEEE Electromagnetic Compatibility Society,* vol. 57, no. 4, pp. 754-763, 2015.

[57] J. Bai, G. Zhang, A. P. A. P. Duffy and L. Wang, "Dimension-Reduced Sparse Grid Strategy for a Stochastic Collocation Method in EMC Software," *IEEE Transactions on Electromagnetic Compatibility,* vol. 60, no. 1, pp. 218-224, 2018.

[58] M. Liu and S. Liu, "Adaptive sparse grid method for RCS estimation of object with uncertain shape," *Electronics Letters,* vol. 46, no. 2, pp. 857-858, 2010.

[59] H. Bagci, A. C. Yucel, J. S. Hesthaven and E. Michielssen, "A Fast Stroud-Based Collocation Method for Statistically Characterizing EMI/EMC Phenomena on Complex Platforms," *IEEE Transactions on Electromagnetic Compatibility,* vol. 51, no. 2, pp. 301-311, 2009.

[60] A. Prasad and S. Roy, "Multidimensional Variability Analysis of Complex Power Distribution Networks via Scalable Stochastic Collocation Approach," *IEEE Transactions on Components, Packaging and Manufacturing Technology,* vol. 5, no. 11, pp. 1656-1668, 2015.

[61] Z. Zhang, T. Weng and L. Daniel, "Big-Data Tensor Recovery for High-Dimensional Uncertainty Quantification of Process Variations," *IEEE Trans. on Components, Packaging and Manufacturing Technology,* vol. 7, no. 5, pp. 687-697, 2017.

[62] P. Manfredi, *High-Speed Interconnect Models with Stochastic Parameter Variability, PhD Thesis,* Torino, Italy: Politecnico di Torino, Porto Institutional Repository, 2013.

[63] P. Manfredi, D. Vande Ginste, I. S. Stievano and F. G. Canavero, "Stochastic transmission line analysis via polynomial chaos methods: an overview," *IEEE Electromagnetic Compatibility Magazine,* vol. 6, no. 3, pp. 77-84, 2017.

[64] M. Larbi, I. S. Stievano, F. G. Canvaero and P. Besnier, "Variability Impact of Many Design Parameters: The Case of a Realistic Electronic Link," *IEEE Transactions on Electromagnetic Compatibility,* vol. 60, no. 1, pp. 34-41, 2018.

[65] A. K. Prasad and S. Roy, "Accurate Reduced Dimensional Polynomial Chaos for Efficient Uncertainty Quantification of Microwave/RF Networks," *IEEE Transactions on Microwave Theory and Techniques,* vol. 65, no. 10, pp. 3697-3708, 2017.

[66] A. K. Prasad and S. Roy, "Reduced Dimensional Chebyshev-Polynomial Chaos Approach for Fast Mixed Epistemic-Aleatory Uncertainty Quantification of Transmission

Line Networks," *IEEE Transactions on Components, Packaging and Manufacturing Technology,* vol. Early Access, pp. 1-1, 2018.

[67] A. Petrocchi, A. Kaintura, G. Avolio, D. Spina, T. Dhaene, A. Raffo, M. M. Dominique and P. Schreurs, "Measurement Uncertainty Propagation in Transistor Model Parameters via Polynomial Chaos Expansion," *IEEE Microwave and Wireless Components Letters,* vol. 27, no. 6, pp. 572-574, 2017.

[68] R. Hu, V. Monebhurrun, R. Himeno, H. Yokota and F. Costen, "An Adaptive Least Angle Regression Method for Uncertainty Quantification in FDTD Computation," *IEEE Transactions on Antennas and Propagation,* vol. 66, no. 12, pp. 7188-7197, 2018.

[69] Y. Wang, S. Jin, S. Penugonda, J. chen and J. Fan, "Variability Analysis of Crosstalk Among Differential Vias Using Polynomial-Chaos and Response Surface Methods," *IEEE Transactions on Electromagnetic Compatibility,* vol. 59, no. 4, pp. 1368-1378, 2017.

[70] O. Alkhateeb and N. Ida, "Data-Driven Multi-Element Arbitrary Polynomial Chaos for Uncertainty Quantification in Sensors," *IEEE Transactions on Magnetics,* vol. 54, no. 3, 2018.

[71] H. Acikgoz and R. Mittra, "Stochastic Polynomial Chaos Expansion Analysis of a Split-Ring Resonator at Terahertz Frequencies," *IEEE Transactions on Antennas and Propagation,* vol. 66, no. 4, pp. 2131-2134, 2018.

[72] Z. Fei, Y. Huang, J. Zhou and C. Song, "Numerical Analysis of a Transmission Line Illuminated by a Random Plane-Wave Field Using Stochastic Reduced Order Models," *IEEE Access,* vol. 5, pp. 8741 - 8751, 2017.

[73] Z. Fei, Y. Huang, J. Zhou and Q. Xu, "Uncertainty Quantification of Crosstalk Using Stochastic Reduced Order Models," *IEEE Transactions on Electromagnetic Compatibility,* vol. 59, no. 1, pp. 228 - 239, 2017.

[74] C. Gabriel, "Compilation of the dielectric properties of body tissues at RF and microwave frequencies,," Technical Report: AL/OE-TR-1996-0037, TX: Brooks Air Force Base; 1, 1996..

[75] C. Gabriel and A. Peyman, "Dielectric measurement: error analysis and assessment of uncertainty," *Physics in Medicine & Biology,* vol. 51, no. 23, 2006.

[76] A. Bahr, T. Bolz, T and C. Hennes, "Numerical Dosimetry ELF: Accuracy of the Method, Variability of Models and Parameters, and the Implication for Quantifying Guidelines," *Health Physics,* vol. 92, no. 6, pp. 521-530, 2007.

[77] M. Murbach, E. Neufeld, W. Kainz, K. P. Pruessmann and N. Kuster, "Whole-body and local RF absorption in human models as a function of anatomy and position within 1.5T MR body coil," *Magnetic Resonance in Medicine,* vol. 71, no. 2, pp. 839-845, 2013.

[78] E. Chiaramello, M. Parazzini, S. Fiocchi, P. Ravazzani and J. Wiart, "Assessment of Fetal Exposure to 4G LTE Tablet in Realistic Scenarios: Effect of Position, Gestational Age, and Frequency," *IEEE Journal of Electromagnetics, RF and Microwaves in Medicine and Biology,* vol. 1, no. 1, pp. 26-33, 2017.

[79] O. Jawad, D. Lautru, J. M. Dricot, F. Horlin, A. Benlarbi-Delaï and P. De Doncker, "Estimation of specific absorption rate with kriging method," in *USNC-URSI Radio Science Meeting*, Lake Buena Vista, FL, USA, 2013.

[80] S. Azzi, Y. Huang, B. Sudret and J. Wiart, "Random Processes Metamodeling Applied to Dosimetry," in *2nd URSI Atlantic Radio Science Meeting (AT-RASC)*, Meloneras, Spain, 2018.

[81] J. Wiart, Radio-Frequency Human Exposure Assessment: From Deterministic to Stochastic Methods, London, UK; Hoboken, NJ, USA: John Wiley & Sons, Inc., 2016.

[82] J. Wiart, P. Kersaudy, A. Ghanmi, N. Varsier, A. Hadjem and P. Odile, "RF Exposure Assessment of Children's Organs using surrogate model built with electromagnetic solvers and Statistics," in *European Conference on Antennas and Propagation (EuCAP)*, Lisbon, Portugal, 2015.

[83] E. Chiaramello, M. Parazzini, S. Fiocchi, P. Ravazzani and J. Wiart, "Stochastic Dosimetry Based on Low Rank Tensor Approximations for the Assessment of Children Exposure to WLAN Source," *IEEE Journal of Electromagnetics, RF and Microwaves in Medicine and Biology,* vol. 2, no. 2, pp. 131-137, 2018.

[84] X. Cheng and V. Monebhurrun, "Application of Different Methods to Quantify Uncertainty in Specific Absorption Rate Calculation Using a CAD-Based Mobile Phone Model," *IEEE Transactions on Electromagnetic Compatibility,* vol. 59, no. 1, pp. 14-23, 2017.

[85] L. Zilberti, D. Voyer, O. Bottauscio, M. Chiampi and R. Scorretti, "Effect of Tissue Parameters on Skin Heating Due to Millimeter EM Waves," *IEEE Transactions on Magnetics,* vol. 51, no. 3, 2015.

[86] R. Gaignaire, R. Scorretti, R. V. Sabariego and C. Geuzaine, "Stochastic Uncertainty Quantification of Eddy Currents in the Human Body by Polynomial Chaos Decomposition," *IEEE Transactions on Magnetics,* vol. 48, no. 2, pp. 451-454, 2012.

[87] S. Lallechere, P. Bonnet and F. Paladian, "Electrical stochastic modeling of cell for bio-electromagnetic compatibility applications," *Annales des Télécommunications,* vol. 69, no. 5-6, pp. 295-308, 2014.

[88] K. Weise, L. Di Rienzo, H. Brauer, J. Haueisen and H. Toepfer, "Uncertainty Analysis in Transcranial Magnetic Stimulation Using Nonintrusive Polynomial Chaos Expansion," *IEEE Transactions on Magnetics,* vol. 51, no. 7, 2015.

[89] L. Codecasa, L. Di Rienzo, K. Weise, S. Gross and J. Haueisen, "Fast MOR-Based Approach to Uncertainty Quantification in Transcranial Magnetic Stimulation," *IEEE Transactions on Magnetics,* vol. 52, no. 3, 2016.

[90] L. Codecasa, L. Di Rienzo, K. Weise and J. Hausien, "Uncertainty quantification in transcranial magnetic stimulation with correlation between tissue conductivities," in *International Applied Computational Electromagnetics Society Symposium (ACES)*, Florence, Italy, 2017.

[91] L. J. Gomez , A. C. Yücel, L. Hernandez-Garcia, S. F. Taylor and E. Michielssen, "Uncertainty Quantification in Transcranial Magnetic Stimulation via High-Dimensional Model Representation," *IEEE Transactions on Biomedical Engineering,* vol. 62, no. 1, pp. 361-372, 2015.

[92] C. Li and T. Wu, "Impact of uncertain transcranial magnetic stimulation coil position and orientation in the stimulation for a motor cortex," in *XXXIInd General Assembly and Scientific Symposium of the International Union of Radio Science (URSI GASS)*, Montreal, QC, Canada, 2017 .

[93] R. Aboulaich, N. Fikal, E. El Guarmah and N. Zemzemi, "Stochastic Finite Element Method for Torso Conductivity Uncertainties Quantification in Electrocardiography Inverse Problem," *Mathematical Modelling of Natural Phenomena,* vol. 11, no. 2, pp. 1-19, 2016.

[94] C. Schmidt, U. Zimmermann and U. Van Rienen, "Modeling of an Optimized Electrostimulative Hip Revision System Under Consideration of Uncertainty in the

Conductivity of Bone Tissue," *IEEE Journal of Biomedical and Health Informatics,* vol. 19, no. 4, pp. 1321-1330, 2015.

[95] A. Arduino, M. Chiampi, F. Pennecchi, L. Zilberti and O. Bottauscio, "Monte Carlo Method for Uncertainty Propagation in Magnetic Resonance-Based Electric Properties Tomography," *IEEE Transactions on Magnetics,* vol. 53, no. 11, 2017.

[96] C. Merla, M. Liberti, F. Apollonio, C. Nervi and G. d'Inzeo, "A 3-D Microdosimetric Study on Blood Cells: A Permittivity Model of Cell Membrane and Stochastic Electromagnetic Analysis," *IEEE Transactions on Microwave Theory and Techniques,* vol. 58, no. 3, pp. 691-698, 2010.

[97] J. J. W. Lagendijk, "Hyperthermia treatment planning",," *Physics in Medicine & Biology,* vol. 45, no. 5, 2000.

[98] A. Šušnjara, D. Poljak, F. Rezo and J. Matković, "Stochastic Sensitivity Analysis of Bioheat Transfer Equation," in *URSI EM Theory Symposium (EMTS)*, San Diego, CA, USA, 2019.

Abbreviation list

ANOVA	ANalysis Of VAriance
BIOEM	bioelectromagnetism
CEM	computational electromagnetism
EMC	electromagnetic compatibility
MC	Monte Carlo
OAT	one-at-a-time
gPC	generalized polynomial chaos
SA	sensitivity analysis
SC	stochastic collocation
(E)SROM	(extended) stochastic reduced order model
UP	uncertainty propagation
UQ	uncertainty quantification

Abstract

Models used to simulate the interaction of electromagnetic fields with physical objects and the environment are mostly deterministic thus providing the result only for a specific setup of input parameters. However, some areas in computational electromagnetics (CEM) suffer from inherent uncertainties of the input parameters resulting in the uncertainties in the assessment of the related response. It is necessary to assess the stochastic output quantities in terms of stochastic moments (mean and variance), probability distributions, confidence intervals, etc. Moreover, in order to gain a better insight into the relationship between the input parameters and the output of interest, a sensitivity analysis of input parameters needs to be carried out.

Traditional methods for uncertainty propagation are easy to implement as they rely upon statistical approaches, e.g. brute force Monte Carlo (MC) sampling. However, despite the fact that the sample size does not depend on random dimension, it still needs to be very high. Therefore, the non-statistical UQ methods have become of interest to researchers in this area. Contrary to statistical, the non-statistical approaches aim to represent the unknown stochastic solution as a function of random input variables. The nature of these methods can be intrusive or nonintrusive. The intrusiveness implies a more demanding implementation since new codes need to be developed, while the non-intrusive methods enable the use of previously validated deterministic models as black boxes in stochastic computations. Both approaches exhibit fast convergence and high accuracy under different conditions.

The goal of this work is to outline some of the most popular UQ methods in CEM as well as to give a state of the art for UQ analysis in the CEM and bioelectrmagnetism. The basic concepts of three uncertainty propagation methods are given: generalized polynomial chaos (gPC), stochastic collocation method (SCM) and stochastic reduced order model (SROM) method. Furthermore, this work investigates the “one-At-a-Time” (OAT) and the “Analysis Of Variance” (ANOVA) based approaches for sensitivity analysis. Finally, an example of UQ for the stochastic bioheat transfer equation is given, thus demonstrating the efficiency of stochastic collocation method w.r.t. MC method.

Sažetak

Matematički i računalni modeli koji se koriste za simulaciju interakcije elektromagnetskih polja i fizičkih objekata uglavnom su determinističke prirode pa tako daju rezultate koji vrijede samo za jedan specifičan set ulaznih parametara. Međutim, neka područja računalnog elektromagnetizma podložna su utjecaju nesigurnosti pristunih kod ulaznih parametara pa tako i izlazne veličine od interesa rezultiraju vrijednostima koje se rasipaju oko određene srednje/očekivane vrijednosti. Potrebno je, dakle, razviti matematički model koji omogućava proračun stohastičkih vrijednosti izlaznih parametara kao što su stohastički momenti: srednja vrijednost i varijanca, zatim distribucija gustoće vjerojatnosti, intervali pouzdanosti, itd. Štoviše, kako bi se dobio bolji uvid u odnos ulaznih i izlaznih parametara, potrebno je provesti analizu osjetljivosti.

Tradicionalne metode za propagaciju nesigurnosti od ulaznih prema izlaznim parametrima, vrlo je lako implementirati budući da se oslanjaju na tzv. statističke pristupe kao što je npr. uzorkovanje Monte Carlo (MC). Međutim, usprkos činjenici da kod statističkih pristupa veličina uzorka ne ovisi o broju ulaznih parameara koji su nasumične prirode, sam uzorak treba biti jako velik, stoga su u posljednjih nekoliko desetljeća ne-statističke metode postale predmet interesa za mnoge istraživače u području računalnog elektromagnetizma (eng. *computational electromagnetics,* CEM), kao i u drugim granama znanosti. Sama priroda ne-statističkih metoda može biti intruzivna i neintruzivna. Intruzivnost podrazumijeva zahtjevniju implementaciju budući da je potrebno mijenjati postojeće determinističke kodove i njihova prilagodba stohastičkim metodama. S druge strane, neintruzivni pristup omogućava ponovnu upotrebu prethodno validiranih i testiranih determinističkih kodova u stilu "crne kutije". Oba ne-statistička pristupa rezultiraju brzom konvergencijom i preciznošću u različitim primjenama.

Cilj ovog rada je predstaviti neke od najpopularnijih metoda za kvantificiranje nesigurnosti (eng. *uncertainty quantification*, UQ) u području računalnog elektromagnetizma kao i dati pregled literature s najvažnijim radovima (eng. *state of the art*) na tu temu. Obrađeni su osnovni koncepti triju metoda za UQ: popopćeni polinomni kaos (eng. *generalized polynomial chaos, gPC*), metoda stohastičke kolokacije (eng. *stochastic collocation,* SC) i stohastički modeli sniženog reda (eng. *stochastic reduced order model*). Nadalje, u ovom radu se istražuju dva pristupa analizi osjetljivosti, tzv. "jedan-po-jedan" pristup (eng. *"one-at-a-time",* OAT) i pristup temeljen na "analizi varijance" (eng. *"analysis of variance"*, ANOVA). Konačno, dan je i primjer kvantifikacije nesigurnosti stohastičke jednadžbe prijenosa topline u biološkom

tkivu, u kojem je demonstrirana efikasnost metode stohastičke kolokacije u odnosu na metodu Monte Carlo.